MCP Papers in Press. Published on December 18, 2007 as Manuscript M700321-MCP200

Quantitative Analysis of Snake Venoms Using Soluble Polymer-based Isotope Labeling

Jacob A. Galan[1], Minjie Guo[1], Elda E. Sanchez[2], Esteban Cantu[2], Alexis Rodriguez - Acosta[3], John C. Perez[2], and W. Andy Tao[1*]

[1]Departments of Biochemistry, Chemistry, Medicinal Chemistry & Molecular Pharmacology, Purdue University, West Lafayette, Indiana 47907 USA.

[2]Natural Toxins Research Center, College of Arts and Science, Texas A&M University-Kingsville, MSC 158, Kingsville, TX 78363 USA.

[3]Immunochemistry Section, Tropical Medicine Institute, Universidad Central de Venezuela, Caracas, Venezuela

[*]Corresponding author:

E-mail: watao@purdue.edu
Tel: (765) 494-9605

Running Title: Quantitative Snake Venom Proteomics

ABBREVIATIONS

SoPIL: Soluble Polymer-based Isotope Labeling

SILAC: Stable Isotope Labeling using Amino acids in Cell culture

iTRAQ: isobaric Tagging for Relative and Absolute Quantitation

PAMAM: Polyamidoamine

SVMP: Snake Venom Metalloproteases

PLA 2: Phospholipases A_2

MTX-A: Mojave toxin (acidic subunit)

MHD: The Minimal Hemorrhagic Dose (minimal protein amount that will cause a 10 mm hemorrhagic spot)

Summary

We present the design and synthesis of a new quantitative strategy termed Soluble Polymer-based Isotope Labeling (SoPIL) and its application as a novel and inclusive method for the identification and relative quantification of individual proteins in complex snake venoms. The SoPIL reagent selectively captures and isolates cysteine-containing peptides, and the subsequent tagged peptides are released and analyzed using nanoflow liquid chromatography-tandem mass spectrometry. The SoPIL strategy was used to quantify venom proteins from two pairs of venomous snakes; *Crotalus scutulatus scutulatus* type A, *C. s. scutulatus* type B, *C. o. helleri*, and *B. colombiensis*. The hemorrhagic, hemolytic, clotting ability and fibrinogenolytic activities of crude venoms were measured and correlated with difference in protein abundance determined by the SoPIL analysis. The SoPIL approach could provide an efficient and widely applicable tool for quantitative proteomics.

Introduction

The identification and accurate quantification of proteins in high throughput analysis are essential components of proteomic strategies for biomarker discovery and studying cellular functions and processes (1) (2). Although the technology to measure mRNA expression is more established, the measurement of differential protein expression provides a more direct, accurate, and versatile way to detect global changes in cellular dynamics in health and disease (3). Over the past several years, many quantitative techniques and strategies have been introduced and thoroughly examined. The traditional and frequently used method to investigate differential protein abundances on a large scale between samples from different sources is the staining of proteins separated by two-dimensional polyacrylamide gel electrophoresis (2D-PAGE). This method falls short in its reproducibility and its inability to detect low abundant and hydrophobic proteins (4). Recently label-free approaches, primarily based on the use of liquid chromatography (LC) and highly accurate mass spectrometers have been investigated (5,6). These methods, however, rely heavily on computational software for data treatment.

Stable isotopic labeling has remained the most popular method for quantitative proteomics. The introduction of stable isotopes has typically been carried out by i) chemical derivatization of proteins or peptides, e.g. via the isotope coded affinity tag (ICAT) (7), isobaric tagging for relative and absolute quantitation (iTRAQ) (8), and isotope coded protein labelling (ICPL)(9) methods; ii) enzyme catalyzed labeling, e.g., proteolysis in heavy water incorporates ^{18}O into the newly-generated C-terminal carboxyl groups (10); and iii) metabolic labeling methods to incorporate isotopically labeled amino

acid residues into proteins (stable isotope labeling using amino acids in cell culture, SILAC) (11). ICAT is probably the best described chemical approach. Over the years, both advantages and disadvantages of ICAT have been recognized. Several variations and modifications of ICAT have been attempted to make it more practical and simpler, such as acid-cleavable ICAT reagents (12) and a solid- phase based version (13). The adaptation of solid-phase capture and release process is a significant improvement and the method obviates extra purification steps and has the potential for automation and high throughput experiments. A side-by-side comparison with the ICAT method demonstrated that the solid-phase method for stable isotope tagging of peptides is comparatively simpler, more efficient, and more sensitive. However, the most notable disadvantages of the solid phase extraction are the heterogeneous reaction conditions that can exhibit nonlinear kinetic behavior, unequal distribution and/or access to the chemical reaction, and solvation problems. The heterogeneous nature of solid-phase reaction for proteomics research presents a serious issue for sample recovery and identification, which usually deals with a small amount of proteins and peptides in extremely complex mixtures.

We attempt to address this issue by the introduction of a new quantitative strategy and reagents, termed Soluble Polymer-based Isotope Labeling (SoPIL). The new reagents are based on soluble nanopolymers such as dendrimers. Dendrimers are a class of hyperbranched synthetic polymers. Built from a series of branches around an inner core, they provide products of different generations and offer intriguing applications (14). Dendrimers are authentic nanoparticles with the dimensions in the range of 2 to 10 nm.

Dendrimers have extremely well-defined cascade motif with a number of characteristics which make them useful in combinatorial chemistry and biological systems. A number of dendrimer types have been used as drug candidates for receptor–ligand interactions, drug carriers for conferring biosurvival, membrane permeability and targeting, and have found wide use as carriers for vaccine antigens (14). We introduced dendrimers to proteomics research for the first time in protein phosphorylation analysis (15), but the application of dendrimers in quantitative proteomics, and potentially in vivo proteomics, is still in its early development (16). New applications for dendrimers open an exciting area for proteomics research that will provide a simple and effective alternative to currently available quantitative technologies.

Snake venoms contain complex mixtures of secreted proteins belonging to many different classes such as neuro-toxins, kappa toxins, cardiotoxins, myotoxins, hemorrhagins, and disintegrins (17). These same proteins that cause tissue damage and trauma when animals or humans are envenomed are also of medical and pharmacological importance. A number of drugs have been derived from snake venom. For example, Ancrod from venom of the Malayan pit viper is a fibrinogenolytic enzyme that is used to treat patients after myocardial infarction (18); Aggrastat (trade name Tirofiban), first isolated from the venom of the Saw-scaled viper, has antiplatelet and anticancer properties (18). Many North American and South American rattlesnakes venoms possess an abundant sources of these medically relevant proteins, and new proteins and their activities are being characterized steadily.

One of the most abundant classes of proteins in snake venom is the hemorrhagic toxins. The snake venom hemorrhagic toxins are metalloproteinases (SVMP) that are characterized according to structural domains, such as subclass P-I, P-II, P-III and P-IV which bear structural similarity to either metalloproteinase alone or have domains similar to disintegrins or c-type lectins (19-21). These are zinc-containing metalloproteases characterized by the presence of a protease domain, with additional disintegrins or c-type lectins domains in some of them. They act by degrading the component proteins of the basement membrane underlying capillary endothelial cells. The toxins also act on these cells causing lysis, resulting in hemorrhage. Some of these toxins have been found to exert additional effects such as fibrino(geno)lysis, and platelet aggregation that facilitate hemorrhage (19).

Another high abundant class of proteins in snake venoms are the phospholipases A_2 (PLA 2), which is a major component in Viperidae/Crotalidae venom. PLA_2 enzymes are single chain polypeptides of around 120 residues or mixtures of 2–5 complementary polypeptides (22). These isoenzymes catalyze the hydrolysis of phospholipids into free fatty acids and lysolipids. PLA_2s display a wide variety of neurotoxic, cardiotoxic, myotoxic, hemolytic, convulsive, anticoagulant, anti-platelet, edema-inducing and tissue-damaging effects (23).

The disintegrins are another important class of molecules that have an active and conserved (RGD or "RGD-like") sequence structural homology that is located around a hairpin loop (24). The RGD-containing disintegrins show differential binding towards the

cell surface receptors known as integrins. Disintegrins can have other active triad motifs (e.g. KGD, MLD, WGD) that bind and inhibit integrins to varying degrees and can play a role in cell-to-matrix or cell-to-cell inhibition (25). The inhibition of integrins can result in altered signal transduction pathways that influence cell migration or adipogenesis, angiogenesis, and other biological events (26-28).

Disintegrins and other snake venom proteins are found in many species of venomous snakes; however, their abundance in venoms varies from snake to snake. Intraspecies and interspecies variations in snake venom make a unique biological source of many different interesting toxins, but these variations are also the cause for ineffective antivenoms. One of the most striking examples of intraspecies variation in rattlesnake venom occurs in the Mohave rattlesnake, *C. s. scutulatus* (29-31).

The analysis of venom by proteomic approaches, such as HPLC or 2D gel electrophoresis combined with mass spectrometry, has increased the identification of proteins in snake venom proteome (9,32-35). Calvete and coworkers analyzed the venoms of the three subspecies of *Sistrurus catenatus* (S. c. *catenatus*, *tergeminus*, and *edwardsii*) and *Sistrurus miliarius barbouri*, by offline reverse phase HPLC, amino terminal sequencing, MALDI-TOF, and CID-MS/MS (33). They observed the difference in the venom composition of closely related species that have different diets. Birrell et al. studied the diversity of venom proteins from 18 of these snake species and the venom protein components were separated by 2DPAGE and identified using mass spectrometry and de novo peptide sequencing (34). These two methods have demonstrated the potential for

comparative venom proteins analysis. To date, little is known about the relative abundance of snake venom proteins existing in different species or in the same species with different geo-origins. Utilizing stable isotope labeling would provide a more detailed and comprehensible analysis for snake venom variation.

The aim of this study was to describe and characterize the novel quantitative proteomics strategy, SoPIL and its applications to examine the venoms from the same species of *C. s. scutulatus* (type A and B) and to examine the venoms from two geographically unrelated snakes *C. o. helleri* and *B. colombiensis* (from North and South America, respectively). Cysteine-containing peptides were efficiently isolated, isotopically labeled, and analyzed by two-dimensional microcapillary LC-tandem mass spectrometry for identification and relative quantification.

Experimental Section

Synthesis of the SoPIL reagents. Unless otherwise noted, chemicals were purchased from Sigma-Aldrich (St. Louis, MO).

*Synthesis of (3,5-Dimethoxy-4-phenylaminomethyl-phenoxy)-butyric acid(**2**).* 4-(4-formyl-3,5-dimethoxyphenoxy)butyric acid (**1**) (Novabiochem, CA) (268 mg, 1.0 mmol) was dissolved in 10 mL DMF and MeOH (1:4 v/v) and mixed with aniline (250 mg, 2.5 mmol) and HOAc (75 μL, 1.25 mmol), followed by the addition of $NaBH_3CN$ (120 mg, 2mmol). The reaction proceeded at room temperature for 2hr and 2 ml H_2O was added, followed by evaporation by vacuum and then the product was extracted with EtOAc and purified by flash chromatography to give NMR pure product 4-(3,5-Dimethoxy-4-

phenylaminomethyl-phenoxy)-butyric acid (**2**) (260 mg, 75%). ^{1}H NMR ($CDCl_3$, 300 MHz): δ 7.17 (t, *J* = 7.5 Hz, 2 H), 6.75 (d, *J* = 7.5 Hz, 2 H), 6.80 (t, *J* = 7.5 Hz, 1 H), 6.10 (s, 2 H), 4.27 (s, 2 H), 4.00 (t, *J* = 6.0 Hz, 2 H), 3.80 (s, 6 H), 2.58 (t, *J* = 7.2 Hz, 2 H), 2.14-2.04 (m, 2 H)

*Synthesis of 4-(4-{[(2-Bromo-acetyl)-phenyl-amino]-methyl}-3,5-dimethoxy-phenoxy)-butyric acid (**3**).* Bromoacetyl chloride (Alfa Aesar) (50 μL, 0.6 mmol) in 0.5 mL anhydrous THF and 0.6 mL of 1N NaOH were added dropwise to the THF solution of compound (**2**) (174 mg, 0.5 mmol) at 0˚C. The reaction was continued at this temperature for 30 min. Then the reaction mixture was neutralized with 1N HCl at 0˚C. The product was exacted with EtOAc and purified by flash chromatography to obtain NMR pure product 4-(4-{[(2-Bromo-acetyl)-phenyl-amino]-methyl}-3,5-dimethoxy-phenoxy)-butyric acid (**3**) (175 mg, 75%). ^{1}H NMR ($CDCl_3$, 300 MHz): δ 7.26-7.21 (m, 3 H), 6.98-6.97 (m, 2 H), 5.92 (s, 2 H), 4.97 (s, 2 H), 3.96 (t, *J* = 6 Hz, 2 H), 3.61 (s, 2 H), 3.59 (s, 6 H), 2.58 (t, *J* = 7.5 Hz, 2 H), 2.11-2.05 (m, 2 H).

The heavy isotope form was synthesized in the same way by using $^{13}C_6$-aniline.

Synthesis of the SoPIL reagents. PAMAM dendrimer Generation 4.0 (28 mg, 2 μmol) was dissolved in 10 mL of 200 mM MES (pH = 5.8) followed by the addition of 4-pentynoic acid (1.6 mg, 16 μmol, 6 equiv per dendrimer) in 200 μL DMF, N-hydroxy succinic anhydride (NHS) (20 mg, 15 mM) and (1-[3-(dimethylamino)propyl] -3-ethylcarbiimide HCl (EDC) (200 mg, 200 mM). The solution was stirred at room temperature for 12 hr. After intensive dialysis in water, the solution was concentrated by

ultrafiltration to 1 mL and split into halves for further reaction with compound (**3**) and the heavy form (**3**)-$^{13}C_{6,}$ respectively. Terminal alkyne functionalized G4-PAMAM (1 μmol) prepared above was dissolved in 2 mL of 200 mM MES (pH = 5.8). Then compound (**3**)-$^{12}C_6$ or -$^{13}C_6$ (9.2 mg, 20 μmol) in 2 mL DMF was added to the above solution followed by the addition of NHS (10 mg, 15 mM) and EDC (100 mg, 100 mM). The reaction was continued at room temperature for 12 hr in the dark. After intensive dialysis in water, the solution was concentrated by ultrafiltration to 600 μL which was directly used for labeling experiments.

Synthesis of azide beads.

1-Amino-11-azido-3,6,9-trioxaundecane (**4**) was prepared as reported in the literature (36). Aminopropyl controlled pore glass beads (200 mg, NH_2: ~400 μmol/g) was mixed with succinic anhydride (80 mg, 0.8 mmol) in 400 μL DMF and 200 μL pyridine. The reaction was allowed to proceed at room temperature overnight, and the beads were extensively washed. 1-Amino-11-azido-3,6,9-trioxaundecane (**4**) (109 mg, 500 μmol) in 500 μL DMF was added to the beads followed by the addition of HOBt (63 mg, 500 μmol) and DIPCI (80 μL, 500 μmol). The reaction was allowed to proceed at room temperature overnight, and the beads were extensively washed and dried in vacuum.

Synthesis of Cys-specific solid phase beads

Aminopropyl controlled pore glass beads (100 mg, NH_2: 400 μmol/g) were pre-washed with anhydrous DMF. 1-hydroxybenzotriazole (25 mg, 200 μmol) in 100 μL DMF, compound (**3**) (92 mg, 200 μmol) in 600 μL DMF and diisopropyl carbodiimide (DIPCI)

(64 μL, 400 μmol) were added to the beads successively for overnight reaction. The beads were then washed sequentially with DMF and dichloromethane and then dried under reduced pressure and stored at room temperature in the dark.

Yield determination of capturing cysteine-containing peptides and acid cleavage reactions using the SoPIL reagent and the direct solid phase approach.

A peptide mixture consisting of 100 pmol cysteine-containing Laminin B (sequence: CDPGYIGSR) and 20 pmol non-cysteine containing angiotensin (sequence: DRVYIHPF) was used. Peptides were reduced with 5 mM tris(carboxyethyl) phosphine (TCEP) in 100 μL of 0.1 M Tris (pH 8.0) and 5 mM EDTA for 10 min at room temperature. Next, 10 nmol SoPIL-$^{12}C_6$ reagent or 7 mg Cys-specific solid phase-$^{13}C_6$ beads were used in parallel to capture peptides in a total volume of 100 μL under constant agitation. Aliquots of 1 μL supernatant were drawn from the reaction mixture for MS analysis before the start of reactions and at different time points during the reaction. After 1 hr of incubation, the reactions were quenched by the addition of 2 μL of 200 mM DTT for 5 min. For the reaction with the SoPIL reagent, 10 mg azide beads were added in a total volume of 400 μL solution containing 2.5 mM TCEP, 2.5 mM $CuSO_4$, 0.25 mM tris(triazolyl)amine for 30 min. Both beads were combined and washed successively by 1M NaCl, H_2O and 80% acetonitrile twice. One hundred microliters of 90% TFA in water was added to the beads and incubate for 1 hr. The released peptides were collected by filtration and beads were washed with 80% acetonitrile twice. The elutions were combined and dried under vacuum for MS analysis. Mass spectra were acquired at the MS mode using a MALDI-TOF/TOF mass spectrometer (ABI 4700, Foster City, CA). Measurements were

performed with 200Hz solid state laser in positive reflector mode with a 2.5 kV acceleration voltage. For each MS spectrum, 1000 laser shots in an m/z window of 800-3000 were accumulated using Data Explorer version 4.2 (Applied Biosystems) software. Mass calibration was achieved using the Sigma calibration kit which includes reference peptides angiotensin I, ACTH, bradykinin, and fibrinopeptide. For sample preparation 0.3 µl of aliquots of the solution were spotted on a target and mixed in 1:1 with a matrix consisting of 80% acetonitrile in water, 0.1% trifluoroacetic acid (TFA), and 7 mg/mL α-cyano-4-hydroxycinnamic acid (CHCA).

Venom Collection

Individual Mohave rattlesnake (*C. s. scutulatus*) type A and B (Avid #011-032-076 and #011-064-358) were collected in Culberson Co., TX, and Pinal Co, Arizona U.S.A, respectively. A Southern Pacific rattlesnake (Avid #011-032-076) was collected from Southern California, San Bernardino Co. These snakes are currently housed at the Natural Toxins Research Center (NTRC), Texas A&M University-Kingsville, Kingsville, TX. The *B. colombiensis* is currently housed at the Instituto de Medicina Tropical, Universidad Central de Venezuela, Caracas. Venom from each snake was extracted in their corresponding locations by allowing the snakes to bite into para-film stretched over a disposable plastic cup. Each venom sample was centrifuged (500 x g for 10 min), filtered through a 0.45 µm filter under positive pressure, and frozen at –90˚C until lyophilized.

Venom Preparation

Fifty microliters of a 10 mg/mL snake venom solutions was prepared was denatured using 8 M urea, and reduced with 5 mM TCEP for 30 min at 37˚C. Urea in the samples was then diluted 4 times with 200 mM Tris, pH 8.5. Twenty micrograms of sequence-graded trypsin (Promega) was added and incubated at 37˚C for 16 hrs. The samples were then dried to 100 µl.

Isotopic labeling and isolation of cysteine-containing peptides

Forty microliters of digested peptide mixture from each sample was labeled with 30 nmol SoPIL reagent. The venom peptides from Mohave type A and Southern Pacific Rattlesnake were labeled using SoPIL-$^{12}C_6$ and venom peptides from Mohave type B and mapanare were labeled with SoPIL-$^{13}C_6$ for 2 hr. Then 20 µL of 200 mM DTT was added to each mixture to quench the excessive bromoacetyl group on the denrimer surface. The two mixtures (Mohave type A and B; Southern Pacific and mapanare) were then mixed together followed by the addition of 130 µl of H_2O, 50 µL of 20 mM tris(triazolyl)amine and 20 µL of 50 mM $CuSO_4$, in a final volume of 400 µL and TCEP, $CuSO_4$, and tris(triazolyl)amine concentration of 2.5 mM, 2.5 mM, and 0.25 mM, respectively. The mixtures were then incubated with 5 mg of azide beads at room temperature for 1 hr. The beads were washed with 50 mM Tris, 1M NaCl, H_2O, and 80% acetonitrile three times, respectively. The beads were incubated with 100 µL 90% TFA for 1hr. The released peptides were collected using filtration and beads were washed with 80% acetonitrile twice. The elutions were combined and dried with a centrifugal speedvac.

Nanoflow LC-MS/MS analysis

The analysis was performed on an Agilent 1100 nanoflow (Agilent Technologies, Wilmington, DE) connected to an LTQ linear ion trap mass spectrometer (ThermoFisher, San Jose, CA). The dried peptides were reconstituted in 16 µL 0.1 % formic acid, and introduced on the nanoflow system with two-dimensional liquid chromatography (SCX and C_{18} reverse phase). The strong cation exchange chromatography (1D) was performed using an Agilent SCX (Zorbax®, 3.5 µ m 35 x 0.3mm, Agilent Technologies) column. The buffer used was 0.1% formic acid with the eluting buffer containing 10 different molar concentrations of 20, 40, 60, 80, 100, 150, 200, 300, 500, 1000 mM of ammonium acetate. The C_{18} reverse phase LC (2D) was performed using an IntegraFrit™ (50 cm x 75 mm) capillary column (New Objectives) packed with 5µm C_{18} Magic® beads (Michrom; 75 µm i.d. and 12 cm of bed length). The electrospray ionization emitter tip was generated with a laser puller (Model P-2000, Sutter Insrument Co.). The mass spectrometer was operated in the data-dependent mode, in which a full scan MS was followed by MS/MS scans of the 10 most abundant ions with +2 to +3 charge states. The mass exclusion time was 180s.

Data analysis

The MS/MS data were converted to a mzXML format using the open-source Trans-Peptide Pipeline (TPP) software (Version 2.9.4), and the resulting mzXML files were searched against Swiss Protein database (Version 43.0 with 146,720 entries) using the SEQUEST™ algorithm on the Sorcerer™ IDA server (Software Version 2.5.6; SageN, Inc, San Jose, CA). Peptide mass tolerance was set at 3.0 amu, and MS/MS tolerance

was set internally by the software with the values varying from 0 up to 1 amu. Search criteria included a static modification of cysteine residue of 133 Da (mass of cysteine plus light SoPIL reagent tag) and a variable modification of 6 Da for cysteines (for the heavy SoPIL reagent tag) and methionine oxidation (16 Da). Searches were performed with semi-tryptic digestion and allowed maximum 2 missed cleavages on the peptides analyzed from the sequence database. The validation of protein identification and quantification were performed with the Transproteomic pipeline (TPP) software. The TPP software includes a peptide probability score program PeptideProphet (37) that aids in the assignment of peptide MS spectrum, and the ProteinProphet program that assigns and groups peptides to a unique protein or a protein family if the peptide is shared amongst several isoforms (38). Since snake genome has not been sequenced and snake venom has a high sequence homology in the cysteine containing region, a number of peptides belong to more than a single protein. ProteinProphet (38) partially solved the problem by grouping all identified peptides and adjusting corresponding probability score. However, based on current knowledge in snake venom there are still quite a few ambiguous cases and therefore peptides were assigned to multiple protein identifications (Supplementary Tables 1-4). PeptideProphet program uses various SEQUEST scores (e.g., Xcorr) and a number of other parameters to calculate a probability score for each identified peptide. PeptideProphet allows filtering of large-scale data sets with assessment of predictable sensitivity and false positive rates (FPR). A PeptideProphet and ProteinProphet threshold of 0.9 probability score was used for all accepted SoPIL-labeled peptide identifications and protein assignment (the estimated FPR is 1.1% for probability score of 0.9). Peptide quantifications were analyzed using ASPARatio software (39)

which reconstructes ion chromatograms from SoPIL-labeled peaks and performes automated statistical analysis of peptide abundance ratios. The ASAPRatio program reconstructs a raw single-ion chromatogram by summing all ion intensities within an *m*/*z* range covering the first three theoretical isotopic peaks of the peptide and over the chromatographic elution period of the peptide. It then applies the Savitzky-Golay smooth filtering method to obtain a smoothed chromatogram. The peptide elution peak is identified along with the corresponding peak center and peak width from the smoothed chromatogram (39). The quantification of peptides identified in different SCX elutions was averaged with manual inspection. All quantified peptides were manually inspected and verified for authenticity. Information about PeptideProphet, ProteinProphet, and ASAPRatio programs and other programs in Transproteomic Pipeline can be found at http://tools.proteomecenter.org/software.php.

Hemorrhagic Assay.

The method of Omori-Satoh et al. (40) was used to determine the minimal hemorrhagic dose (MHD) for the crude venoms. One milligram per milliliter solution was prepared for each snake venom. Eight one-half series dilutions were prepared for the snake venoms (1-1/256), of which 0.1 mL of each dilution was injected intracutaneously into the depilated backs of rabbits. After 24 h, the rabbit was sacrificed and the skin removed. A caliper was used to measure the hemorrhagic diameter on the skin and the MHD was determined. The MHD is defined as the amount of venom protein that causes a 10 mm hemorrhagic spot.

Sonoclot Analyzer Profiles

A glass bead activated test (gbACT + Kit obtained from Sienco, Inc.) was used to monitor the effect of venoms on human blood coagulation on a Sonoclot® Coagulation and Platelet Function Analyzer (Sienco, Inc.) according to Sanchez et al (31). Data acquisition and analysis were performed with Signature Viewer software (Sienco, Inc.).

Removal of serine proteases from crude venoms. A HiTrap Benzamidine FF (high sub) column was used to remove the serine proteases from the crude venoms. One milliliter (5 mg/mL) venom samples in 0.05M Tris-HCl, 0.5M NaCl pH 7.5 was added to a 1 mL HiTrap column using a 1-mL luer lock syringe. The serine proteinase free venom was washed out using 0.05M Tris-HCl, 0.5M NaCl, pH 7.5. The serine proteinases were eluted off with 0.01M HCl, 0.5M NaCl, pH 2.0 in 1 mL aliquots in eppendorf tubes containing 70 µL of 1M Tris-HCl, pH 9.0.

Fibrinogenolytic assay

Fibrinogenolytic activity of crude and serine protease free snake venom (0.03 mg/mL) was determined using 12% Tris-Glycine gels on a Power Pac Basic™ (Bio-rad Laboratories, Hercules, CA). Twenty microliters of fibrinogen solution at 2.5 mg/mL in 0.05M Tris-HCl, pH 7.5 containing 0.5M NaCl with 10 µL of the venom samples were incubated at 37˚C for 2 and 24 hr. A total of 12 µL of the fibrinogen/venom mixture was reduced with 6 µL of Tris-Glycine SDS sample buffer (2X) and 2 µL of NuPage sample reducing agent (10X) and boiled for 3 min. The gels were stained with SimplyBlue™

SafeStain (Invitrogen). The proteolytic activity was determined by the disappearance of the α, β, and γ chains of the fibrinogen.

Hemolytic assay

The minimal hemolytic activity of the crude venoms was determined as described by Habermann et al. (41) with modifications. Briefly, 0.3 mL of packed human erythrocytes were washed five times with saline solution, and 0.3 mL of a large, fresh egg yolk diluted 1:4 with saline solution and 0.25 mL of a 0.01M $CaCl_2$ solution were added to 25 mL of 0.8% agarose dissolved in phosphate-buffered saline (PBS) solution (pH 8.1). The mixture was poured into plastic petri dishes (135 x80 mm) and allowed to solidify. After the mixture was solidified, 12 three millimeter diameter wells were prepared and filled with 10 µL of crude venom solution at various concentrations. The plates were incubated at 37˚C for 5 hr and the diameters of the hemolytic haloes were measured. Saline solution and PBS were used as controls. The minimal hemolytic dose was defined as the amount of venom protein that causes a 10 mm halo spot.

Results/Discussion

Rationale for the use of soluble nanopolymer-based reagents for quantitative proteomics. We attempt to address two concerns in existing proteomics research with the SoPIL reagents. The first one is the efficiency and consistency of sample preparation in proteomics research. Sample preparation in proteomics includes the isolation and labeling of a class of proteins/peptides from complex mixtures. Current methods either include extra purification steps that could lead to severe sample loss or solid phase extraction that

is usually limited by heterogeneous reaction and nonlinear kinetics. We address this issue by building the function groups for reaction, isotopic labeling and isolation on a soluble nanopolymer. The soluble polymer, PAMAM dendrimer G4, was functionalized with the reactive group-bromoaceto group for site specific, stable isotopic labeling of cysteine-containing peptides, aniline-$^{12}C_6$ or -$^{13}C_6$ as the isotope tag, and pentynyl group as the "handle" for the isolation of polymer-bound peptides through the highly efficient click chemistry (Scheme 1). The design was based on the concept that specific capture of targeted proteins/peptides, the rate-limiting step, is more efficient to be carried out in the solution phase than on the solid phase, and in the second step, samples tagged with nanopolymers are isolated on a solid phase by choosing a highly efficient bio-conjugation reaction between a pair of bioorthogonal groups on the soluble polymer and on the solid phase (Scheme 2). The high ratio of the reactive group to the handle groups in a homogenous reaction enables us to tag the samples without extra purification steps to remove excessive reagents which are normally required for small chemical reagents such as ICAT reagents.

Soluble nanopolymers such as dendrimers also provide another unique feature for proteomics research. Dendrimers can effectively permeate into living cells and have become one important class of molecules for drug and gene delivery. Although this feature was not explored in this study, SoPIL could address the second concern that *in vitro* proteomic preparations can only, at best, approximate the functional state of proteins in the living cell or organism by achieving proteomics in living cells or *in vivo*.

Characterization and application of the SoPIL method to standard peptide and protein mixtures. We have investigated several types of biologically inert coupling partners functionalized on the PAMAM dendrimer and on the solid phase separately that would react at practical rates at submillimolar concentrations at high yield. We chose to use click chemistry, copper(I) catalyzed azide-alkyne cycloaddition, due to its biocompatibility and high reaction efficiency. The syntheses of SoPIL reagents and azide solid phase beads and the chemical procedure to tag Cys-containing peptides are illustrated in Scheme 1, 3 and 4, respectively. In order to isotopically label and then recover tagged peptides for quantitative mass spectrometry analysis, an acid-cleavable linker 5-(2-formyl-3,5-dimethoxyphenoxy) pentanoic acid (BAL, Backbone Amide Linker) was introduced between dendrimer and the isotope tag.

To demonstrate the SoPIL strategy and to make a parallel comparison between the SoPIL and one-step solid phase methods, we used a standard peptide mixture consisting of a cysteine-containing laminin B (m/z 967) and a non-cysteine containing angiotensin II (m/z 1046) (Fig. 1A). In order to make accurate comparisons, we designed a method based on stable isotope dilution. The standard peptide mixture was allowed to react with the light SoPIL reagent (SoPIL-$^{12}C_6$) and the heavy solid phase reagent (SP-$^{13}C_6$) in parallel. The solid phase reagent was synthesized in a similar fashion to directly incorporate the acid-cleavable linker, the isotope tag aniline, and bromoacetyl group as the thiol-specific group on the aminopropyl controlled pore glass beads (Scheme 3) (See Experimental Section for detailed synthesis). Laminin B was attached to the polymer in less than 1 min after the SoPIL reagent was added into the peptide mixture. In contrast,

only 50% of laminin B was captured on the solid phase during the same time frame and it took over 30min for the solid phase reagent to completely capture the peptide in the solution (Fig. 1 B&C). Both reactions were allowed to go to completion and quenched with 10 mM DTT. The SoPIL reagent was then captured on the azide-functionalized beads through the click chemistry. The resulting beads were combined with solid phase-$^{13}C_6$ beads, washed, and treated with acid. Recovered tagged products were analyzed on the same MS spectrum. The yield using the SoPIL method was over 85% while it was less than 40% for the solid phase method (Fig. 1D). Therefore, the data demonstrated that the capture and release of laminin B using the SoPIL reagent were specific and more efficient than the one-step solid phase isotopic labeling reagent.

To illustrate the quantitative nature of the SoPIL method, a standard protein mixture was used (Table 1). Two mixtures containing the same four proteins (bovine serum albumin, α-lactalbumin, lysozyme C, and β-lactoglobulin) at different concentration ratios were prepared and analyzed as illustrated in Scheme 5. The isolated labeled cysteine-containing peptides were quantified and sequenced using μLC-MS/MS analysis. Using 1-400fmols, all four proteins were explicitly identified with multiple cysteine-containing peptides that accurately quantified with mean differences below 20% between the observed and expected quantities. In addition, the SoPIL reagents efficiently labeled peptides containing more than one cysteine residue, a feature the solid phase method cannot achieve due to steric hindrance (13).

Potential modifications on other amino acid residues (e.g., lysine, histidine, methionine, tryptophan) were examined using differential modifications on these residues during database search (Supplementary Data). No other modifications were identified except cysteine residues, indicating the derivatization using the SoPIL reagents is specific.

Application of the SoPIL method to the quantitative analysis of snake venoms. The SoPIL strategy was applied to study differences in protein abundance in snake venoms. We chose to quantitatively analyze two pairs of snake venoms. The first pair, Mohave rattlesnake venoms type A and B, from the same species, and the second pair, *B. colombiensis* and *C. o. helleri,* two regionally distinctive snakes. Many snake venom proteins are extremely cysteine rich (18), making them an excellent paradigm for us to study using cysteine-specific SoPIL reagents.

Most venom from the Mohave rattlesnakes in the southwestern United States and in Mexico, *C. s. scutulatus* type A venom, are characterized with Mojave toxins and do not induce severe hemorrhage in animals. In contrast, *C. s. scutulatus* type B, found in a narrow range of Arizona, lacks Mojave toxins and has hemorrhagic activity. The same amounts of these two characteristically different snake venoms, C. *s. scutulatus* type A and B, were labeled by light and heavy SoPIL reagents, respectively. They were combined and processed as described in Scheme 4. The analysis identified and quantified over 100 unique peptides representing over 30 venom proteins in Swiss Protein Database (Table 2 for a partial list and a full list in Supplementary Data Table S1 and S2). Relatively low number of identified proteins was due to unsequenced snake genome and

wide dynamic range in venom proteins. Snake venom is dominated by a number of highly abundant proteins. Our analysis also revealed peptide redundancy which could be due to the high sequence homology conserved in the cysteine containing region unique to snake venom. The distribution of identified proteins was illustrated in Fig 2A. Approximately 18% of identified proteins were classified as homologs. Consistent with previous reports on the Mohave rattlesnake, the quantitative measurements indicated that several classes of cysteine-rich proteins dominantly exist in venom A but not in venom B, such as Mojave toxins. The Mohave rattlesnake is an example of extreme intraspecies variation in venom characterization (42). Mohave rattlesnake venom is one of the most toxic snake venoms found in the United States. The lethal dose killing 50% of a mouse population (LD_{50}) ranging between 0.13 and 0.54 mg/Kg body mass (43). This potent lethality is largely due to Mojave toxin, a powerful presynaptically acting neurotoxin that blocks the neurotransmitter acetylcholine resulting in paralysis. Quantitative proteomic analysis determined that the relative intensity of Mojave toxin alpha subunit in the *C. s. scutulatus* type A venom is 15 times more abundant than that in the type B venom (Figs. 3A & B).

Conversely, the disintegrins were only observed in venom B, which was verified in a recent study by Sanchez et al (31). The identification of the disintegrin protein in Mohave type B venom was characterized and showed a strong correlation with the crude venom from these snakes. Hemorrhagic activity for Mohave type B is higher than type A (31). In contrast, Mohave type A did not have the genes for disintegrins and was not hemorrhagic, which was probed with primers design for a highly conserved *C. atrox*

disintegrin gene and analyzed using PCR. This study also demonstrated that the disintegrin protein was also inclusive to Mohave type B venom and not A. The proteomics data showed that type B had more hemorrhagins (venom metalloproteinases), thrombin-like enzymes (serine proteinases), and platelet-aggregating proteinases, which promote and facilitate degradation, hemolysis of cells structural membranes, and inhibition of platelets resulting in tissue damage leading to excessive hemorrhaging. These results were also confirmed by the fibrinogenolytic gels in which both metallo- and serine proteinases were responsible for cleaving the alpha and the beta chain, respectively (Fig. 4A and B). Many thrombin-like enzymes were also found in the Mohave type A venom, such as serine proteinases, venombin A, and calobin. Our results also showed that a snake venom metalloproteinases (SVMP) with a disintegrin domain exist (domain conserved in acostatin-B, piscivostatin-beta, contortrostatin) in the Mohave type A venom. However, the serine proteinases were the ones responsible for the cleavage of the beta chain of fibrinogen (Fig. 4A and B).

The Southern Pacific rattlesnake (*C. o. helleri*) and Mapanare (*B. colombiensis*), which are indigenous to North and South America, respectively, display different venom characterizations. Most *Bothrops* species in South America cause necrosis, hemorrhage and procoagulant activity inducing stroke and myocardial infarction in animals and humans (44); where as many *Crotalus* species have metalloproteinases that cause severe hemorrhages and tissue damage at the site of envenomation (45,46). The same amount of snake venoms of *B. colombiensis* and *C. o. helleri* were also labeled by light and heavy SoPIL reagents, respectively, combined and processed as described in Scheme 4. This

second set for SoPIL analysis identified and quantified similar number of peptides and proteins in Swiss Protein Database (Table 3, Supplementary Data Table S3 and S4). The distribution of identified proteins was illustrated in Fig 2B. Similar to the first Mohave rattlesnake analysis, 22% of identified proteins were classified as homologs.

Myotoxins are typically small proteins and peptides in the snake venom, which upon envenomation, can induce irreversible damage to skeletal muscle fibers (myonecrosis) (47). They are abundant and widespread in South American venomous snakes, but can also be found in the venoms from other species, including the Timber rattlesnake (*C. horridus*) found in North America (48). In the analysis, myotoxins I, II, and III were more abundant in *B. colombiensis* venom than in the *C. o. helleri* venom. In contrast, CAM-toxin, a myotoxin was found in *C. o. helleri* venom. In addition, phospholipase A_2 alpha (Phosphatidylcholine 2-acylhydrolase) was also present in the venom of *C. o. helleri*. These results are consistent with the previous study in which South American *Bothrops* species exhibit increased procoagulant and myotoxic activity compared to many North American *Crotalus* species (49). Neurotoxic PLA_2 myotoxins can also be present in a number of viperid/crotalid species, such as crotoxin a neurotoxin found in the venom of *C. d. terrificus* from South America (50).

The Southern Pacific rattlesnake, *C. o. helleri*, has myotoxic, neurotoxic, and hemorrhagic components in its venom (51,52). French et al (53) reported that Mojave toxin (MT) has been detected in five of 25 *C. o. helleri* using anti-MT antibodies and was confirmed using nucleotide sequence analysis. All of the positive venom samples for MT

were collected from Mt San Jacinto in Riverside Co., California. In our study, no MT was found in the venom of the Southern Pacific venom. Hemorrhagic metalloproteinase HT-E precursors (atrolysin E, D and C) were the most abundant proteins relative to the mapanare venom in addition to adamalysin II (proteinase II). The minimal hemorrhagic dose (minimal protein amount that will cause a 10 mm hemorrhagic spot) for the Southern Pacific venom has been reported to be 2.25 µg (54).

Crude Snake Venom Biological Assays. The biological assays, hemorrhagic, hemolytic, sonoclot, and fibrinogenolytic were carried out on the four crude snake venoms and these assay results were compared with those obtained with the SoPIL method. In the venom of *C. s. scutulatus* type A, the MHD was 162.5 µg, and conversely, type B venom had a MHD of 16 µg. This assay confirms the higher abundance of metalloproteases existing in type B venom relative to A analyzed using the SoPIL method (Table 2). In addition, the hemolytic activity of type B venom was higher than A, possibly due to the higher abundance of most phospholipases found in type B venom, as confirmed by the SoPIL method. Furthermore, the Sonoclot analyzer revealed that Mohave type B venom had a delayed activated clot time of 354s with a low clot rate of 6.2 clot signals/min, while Mohave type A venom displayed a normal activated clot time of 144 s with a low clot rate of 10 clot signals/min (Fig 5A & Table 4). These results are in accordance with the SoPIL method, in which more metalloproteinases were found in type B venom than in type A. Furthermore, the α chain of fibrinogen was cleaved by metalloproteinases found in type B venom, but not in type A venom (Fig. 4A&B). Metalloproteinases inhibit blood coagulation (23), and they can be α- and or β-fibrinogenases depending on their

specificity to cleave the α or β chain of fibrinogen (55). Serine proteinases are other types of proteins found in snake venom that affect platelet aggregation, blood coagulation, fibrinolysis, the complement system, blood pressure, and the nervous system (23,56-62). Serine proteinases were found in slightly higher abundance in Mohave type A venom according to the SoPIL method (Table 2). According to the results in the fibrinogenolytic assay, both type A and B venoms contained serine proteinases that cleaved the β chains (Figs. 4A&B); this was evident when the serine proteinases were removed from these venoms and no cleavage of β chain was observed (Fig. 4B). However, there is further evidence that both metallo- and serine proteinases in both type A and type B venoms are acting complementary on the β chains. For instance, whole venom in 2 hr was able to cleave β chain, but when serine proteinases were removed the β chains remained, leaving the impression that serine proteinases were solely responsible for the β chain cleavage. However, in 24 hr, β chains were completely cleaved with both crude and serine free venom, and it is obvious that metalloproteinases or other enzymes were also responsible for the β chain cleavage in the serine free venom, but required a longer time for the cleavage to occur. Type A venom contains serine proteinase that cleaves the α chain, but also required more time to do so (Figs. 4C&D). These serine proteinases are thrombin-like enzymes, which make blood unclottable, and it is safe to state that type A venom contains different serine proteinases affecting either α or β chain, because it is unlikely that the same serine proteinases could be affecting both chains. (63,64). A combination of both metallo- and serine proteinases exist in a higher abundance in type B venom than in type A venom (Table 2), and thus, the combination of both these proteinases, in

particularly the effect of α chain cleavage by metalloproteinases could very well be the result of the delayed clotting time of blood treated with type B venom (Fig. 5A).

The venoms of *B. colombiensis* and *C. o. helleri* show very distinct coagulant activities from that of the *C. s. scutulatus* venoms (Fig. 5). Both venoms have increased procoagulant activity (Fig. 5), but the mechanism of clotting may be due to different venom proteolytic enzymes affecting different factors of the hemostasis pathway (65). *Bothrops colombiensis* venom cleaves the α, and β, of fibrinogen, where as *C. o. helleri* also cleaves the α chain and partially the β chain. The cleavage of the α and β chains by *B. colombiensis* venom is due to metalloproteinases because when the serine proteinases were removed from the venom, cleavage of both α and β chains still occurred in both 2 and 24 hr incubation periods (Figs. 4A, B, C, &D). Again, cleavage of the β chain by *C. o. helleri* venom may be due to both metallo- and serine proteinases acting synergistically on it. The hemolytic activity was higher in *B. colombiensis* than *C. o. helleri* venom; however, *C. o. helleri* venom was more hemorrhagic. The hemolytic activity is due to phospholipases, while hemorrhaging is due to metallo- and serine proteinases, which by SoPIL analysis phospholipases and metalloproteinases where found in higher abundance in *B. colombiensis* and *C. o. helleri* venoms, respectively (Table 3).

Protease activity in snake venoms. This study also observed for the first time extensive cleavage of venom proteins in all four snake venoms. Tables 5 and 6 illustrate the random protease cleavage of the metalloproteinase jararhagin and metalloproteinase HT-D from the *C. s. scutulatus* and *B. colombiensis*/*C. o. helleri* analysis, respectively. A majority of

peptides have only one tryptic end (22 out of 28 and 13 out of 17 in Table 5 and 6, respectively) and the cleavage was found on every amino acid residue in some peptides. Such extensive cleavage was most likely the result of a combination of activities by multiple proteases in the snake venom. Proteases and other enzymes in snake venom have multiple purposes such as increasing the prey's uptake of toxins and the digest of preys. Such endogenous protease activities in all four venoms could alter the average protein abundance, resulting in relatively large error in any existing measurement method, including the proteomics method.

It is not clear when venom proteases were activated. The activation might occur during the procedure the venoms were collected. After lyophilization and denaturing, the proteases lost their activities. However it is possible that the proteases were reactivated during tryptic digestion period, resulting in extensive cleaves of venom proteins. In addition, it is known that trypsin may result in nonspecific cleavages, even if sequence-graded trypsin was used for better specificity (66).

Conclusion

This study presented the first quantitative proteomic analysis of snake venom from several species based on stable isotope labeling. The new SoPIL reagents that selectively label and isolate cysteine-containing peptides provide a powerful analytical tool to screen snake venoms that are cysteine-rich for many diverse classes of proteins. This new methodology takes the advantage of the homogeneity of solution reaction, high efficiency of click chemistry and convenience of solid-phase capture/release process. The

quantitative proteomics study helps us understand geographical and environmental variations in snake venoms, which is crucial in developing better therapeutic agents for treating snakebites. In addition, quantitative proteomics can also be used for discovering new therapeutic molecules present in snake venom. The conclusions of this study support the theory that there are characteristic differences in the venoms within the same species and from different geographical locations (31). It is evident that the SoPIL method can be an efficient tool for snake venom research and for a much wider application of quantitative proteomics.

Acknowledgments

This project has been funded in part by Purdue University, the American Society for Mass Spectrometry (ASMS) and NSF CAREER development award (to W.A.T.). We thank Professor M. G. Finn in the Scripps Research Institute for the supply of ligand for the click chemistry and for helpful suggestions. We acknowledge the use of software in the Institute for Systems Biology developed using Federal funds from the National Heart, Lung, and Blood Institute, National Institutes of Health, under contract No. N01-HV-28179. This research was also supported by grants to the NTRC at Texas A&M University-Kingsville: NIH/NCRR #1 P40 RR018300-01, NIH/RIMI #5 PMD000216-02, and NIH/SCORE #5 S06 GM008107-29, and grants from FONACIT (G-2005000400). We thank Luis Fernando Navarrete for venom extractions done at the Instituto de Medicina Tropical, Universidad Central de Venezuela.

Table 1. Quantitative analysis of standard protein mixture using the SoPIL reagents.

Protein Name	Peptide sequence[a]	Observed ratio[b]	Mean ± SD	Expected ratio	% error
Bovine serum albumin	K.TC*VADESHAGC*EK.S	1.33 ± 0.22	1.19 ± 0.22	1.0	19
	F.HADIC*TLPDTEK.Q	1.03 ± 0.14			
	K.YIC*DNQDTISSK.L	1.17 ± 0.2			
	R.NEC*FLSHKDDSPDLPK.L	1.44 ± 0.51			
	K.DDPHAC*YSTVFDK.L	1.29 ± 0.24			
	K.EAC*FAVEGPK.L	1.18 ± 0.16			
	K.LKEC*C*DKPLLEK.S	1.61 ± 0.07			
	R.ETYGDMADC*C*EK.Q	1.32 ± 0.21			
	K.SLHTLFGDELC*K.V	0.88 ± 0.15			
	K.EYEATLEEC*C*AK.D	1.12 ± 0.17			
	K.SLHTLFGDELC*K.V	0.88 ± 0.15			
	K.YNGVFQEC*C*QAEDK.G	1.48 ± 0.22			
	K.LFTFHADIC*TLPDTEK.Q	1.15 ± 0.14			
	K.EC*C*HGDLLEC*ADDRADLAK.Y	1.02 ± 0.54			
β-lactoglobulin	L.SFNPTQLEEQC*HI.-	0.62 ± 0.08	0.52 ± 0.11	0.5	4
	R.LSFNPTQLEEQC*HI.-	0.46 ± 0.08			
	F.C*MENSAEPEQSLAC*QC*LVR.T	0.47 ± 0.06			
α-lactalbumin	K.FLDDDLTDDIMC*VK.K	1.9 ± 0.78	2.15 ± 0.43	2.0	8
	K.DDQNPHSSNIC*NISC*DK.F	2.74 ± 0.56			
	H.SSNIC*NISC*DK.F	1.82 ± 0.19			
lysozyme C	L.LSSDITASVNC*AK.K	0.99 ± 0.15	1.07 ± 0.12	1.0	7
	C.SALLSSDITASVNC*AK.K	1.16 ± 0.3			
	R.NLC*NIPC*SALLSSDITASVNC*AK.K	0.94 ± 0.15			
	R.C*ELAAAMK.R	1.22 ± 0.05			

[a]Period indicates a tryptic cleavage site; dash indicates a C-terminal residue.
[b]Ratios ($^{12}C_6/^{13}C_6$) and errors were calculated using the open-source ASAPRatio program.
*indicates the modification of Cys residue by SoPIL reagents.

Table 2. Partial List of Proteins Identified and Relative Abundance in the venom of *C.s. scutulatus* A and B

Entry no.	Protein ID	Description	No. of Identified Peptides	Mean ± SD†
1	gi|13959630|sp|Q91053|VSP1_AGKCA	Calobin precursor	8	1.84 ± 0.76
2	gi|461932|sp|P30403|DISR_AGKRH	Hemorrhagic protein-rhodostomin precursor (RHO) [Contains: Disintegrin rhodostomin (Disintegrin kistrin)	2	0.23 ± 0.08
3	gi|26397690|sp|Q8UVZ7|PA2H_CROAT	Phospholipase A2 homolog Cax-K49 precursor	2	0.51 ± 0.45
4	gi|13959639|sp|Q9DF67|VSP2_TRIJE	Venom serine proteinase 2 precursor (SP2)	6	2.89 ± 0.76
5	gi|6093636|sp|O93364|OXLA_CROAD	L-amino acid oxidase precursor (LAO) (LAAO) (Apoxin I)	18	0.58 ± 0.42
6	gi|27151648|sp|O42188|PA29_AGKHP	Phospholipase A2 homolog	2	<0.05
7	gi|462320|sp|P34182|HRTE_CROAT	Hemorrhagic metalloproteinase HT-E precursor (Atrolysin E) (Hemorrhagic toxin E)	6	0.15 ± 0.46
8	gi|231997|sp|P30431|DISJ_BOTJA	Putative venom metalloproteinase jararhagin precursor (HF2-proteinase) [Contains: Disintegrin]	19	0.25 ± 0.36
9	gi|13959659|sp|Q9YGI6|VSP2_AGKHP	Pallabin 2 precursor	5	2.49 ± 0.97
10	gi|122973|sp|P07973|HEMA_INCEN	Hemagglutinin-esterase precursor [Contains: Hemagglutinin chain 1 (HE1)	1	5.19 ± 0.84
11	gi|13959638|sp|Q9DF66|VSP3_TRIJE	Venom serine proteinase 3 precursor (SP3)	12	0.27 ± 0.52
12	gi|129470|sp|P24027|PA2C_CRODU	Phospholipase A2 CB2 precursor (Crotoxin basic chain 2) (Phosphatidylcholine 2-acylhydrolase)	6	2.66 ± 3.42
13	gi|26007015|sp|P18998|PA2A_CROSS	Mojave toxin acidic chain precursor (Mtx-a)	11	1.35 ± 1.26

14	gi|118651|sp|P21858|DISI_AGKHA	Disintegrin halysin (Platelet aggregation activation inhibitor)	1	0.15 ± 0.02
15	gi|462301|sp|P20164|HR1B_TRIFL	Hemorrhagic metalloproteinase HR1B (Trimerelysin I)	2	0.11 ± 0.13
16	gi|27151653|sp|Q9PVE9|PA2C_AGKRH	Phospholipase A2 S1E6-c precursor (Phosphatidylcholine 2-acylhydrolase)	5	0.07 ± 0.09
17	gi|118652|sp|P16338|DISI_AGKPI	Disintegrin applagin (Platelet aggregation activation inhibitor)	1	<0.05
18	gi|13959631|sp|Q91507|VSP1_TRIMU	Mucrofibrase 1 precursor,Mucrofibrase 3 precursor	3	1.20 ± 0.22
19	gi|118661|sp|P21859|DISI_TRIFL	Disintegrin triflavin (Platelet aggregation activation inhibitor)	7	0.46 ± 0.24
20	gi|129398|sp|P04417|PA21_AGKHA	Phospholipase A2, basic (PA2-I) (Phosphatidylcholine 2-acylhydrolase)	2	<0.05
21	gi|127777|sp|P12028|MYX1_CROVC	Myotoxin I,Myotoxin (Toxic peptide C),Myotoxins 2 and 3,Myotoxin (CAM-toxin)	1	1.39 ± 0.23
22	gi|125179|sp|P15946|KLKB_MOUSE	Glandular kallikrein K11 precursor (Tissue kallikrein) (mGK-11)	1	2.08 ± 2.24
23	gi|27734437|sp|P59171|PA25_ECHOC	Phospholipase A2 5 precursor (Phosphatidylcholine 2-acylhydrolase)	1	0.55 ± 0.03
24	gi|13959617|sp|O13059|VSP1_TRIGA	Venom serine proteinase 1 precursor	3	1.41 ± 0.20
25	gi|13959616|sp|O13058|VSP3_TRIFL	Venom serine proteinase 3 precursor	3	1.79 ± 0.65
26	gi|3122187|sp|P81176|VSP1_AGKHA	Halystase	4	0.04 ± 0.00

†large standard deviation is mainly due to the effect of endogeneous proteolytic activities and degenerate peptides.

Table 3. Partial List of Proteins Identified and Relative Abundance in the venom of *C. o. helleri* and *B. colombiensis*

Entry No.	Protein ID	Description	No. of Identified Peptides	Mean ± SD†
1	gi|34922459|sp|P83519|LECG_BOTJR	Galactose-specific lectin (BJcuL)	2	0.14 ± 0.04
2	gi|6093636|sp|O93364|OXLA_CROAD	L-amino acid oxidase precursor (LAO) (LAAO) (Apoxin I)	17	3.61 ± 2.42
3	gi|1171971|sp|P45881|PA21_BOTJR	Phospholipase A2 precursor (Phosphatidylcholine 2-acylhydrolase) (BJUPLA2)	7	0.13 ± 0.21
4	gi|27151652|sp|O42192|PA28_AGKHP	Phospholipase A2 A' (Phosphatidylcholine 2-acylhydrolase)	4	0.40 ± 0.58
5	gi|13959633|sp|Q91509|VSP3_TRIMU	Mucrofibrase 3 precursor,	2	1.45 ± 0.75
6	gi|584725|sp|P34179|ADAM_CROAD	Adamalysin II (Proteinase II)	8	2.18 ± 2.00
7	gi|231997|sp|P30431|DISJ_BOTJA	Putative venom metalloproteinase jararhagin precursor (HF2-proteinase) [Contains: Disintegrin]	21	2.53 ± 4.56
8	gi|13959659|sp|Q9YGI6|VSP2_AGKHP	Pallabin 2 precursor	4	0.24 ± 0.87
9	gi|27734229|sp|P81509|CHBB_CROHO	CHH-B beta subunit	6	8.39 ± 12.2
10	gi|118651|sp|P21858|DISI_AGKHA	Disintegrin halysin (Platelet aggregation activation inhibitor)	1	1.37 ± 0.15
11	gi|13959630|sp|Q91053|VSP1_AGKCA	Calobin precursor	6	0.75 ± 0.45
12	gi|6093643|sp|P81824|VSP1_BOTJA	Platelet-aggregating proteinase PA-BJ	3	0.05 ± 0.02
13	gi|13959639|sp|Q9DF67|VSP2_TRIJE	Venom serine proteinase 2 precursor (SP2)	4	10.9 ± 9.52
14	gi|118655|sp|P18618|DISI_BOTAT	Disintegrin batroxostatin (Platelet aggregation activation inhibitor)	3	3.06 ± 2.00
15	gi|1171973|sp|P24605|PA22_BOTAS	Phospholipase A2 homolog 2 (Myotoxin II)	20	0.07 ± 0.12
16	gi|129400|sp|P20474|PA21_BOTAS	Phospholipase A2 (Myotoxin I) (Phosphatidylcholine 2-acylhydrolase)	9	0.12 ± 0.17

17	gi|127786|sp|P24330|MYX_CROAD	Myotoxin (CAM-toxin)	4	0.44 ± 1.09
18	gi|1708301|sp|P15167|HRTD_CROAT	Hemorrhagic metalloproteinase HT-D and HT-C precursor (Atrolysins D and C) (Hemorrhagic toxins C and D)	11	>20
19	gi|462320|sp|P34182|HRTE_CROAT	Hemorrhagic metalloproteinase HT-E precursor (Atrolysin E) (Hemorrhagic toxin E)	5	10.9 ± 7.28
20	gi|462318|sp|P20897|HRT2_CRORU	Hemorrhagic metalloproteinase HT-2 (Ruberlysin) (Hemorrhagic toxin II)	16	15.0 ± 31.1
21	gi|461512|sp|P09872|VSP1_AGKCO	Ancrod (Venombin A) (Protein C activator) (ACC-C)	3	1.47 ± 0.50
22	gi|129507|sp|P00623|PA2_CROAD	Phospholipase A2 alpha (Phosphatidylcholine 2-acylhydrolase)	5	1.51 ± 0.45
23	gi|118660|sp|P17349|DISI_TRIEL	Disintegrin elegantin (Platelet aggregation activation inhibitor)	7	3.40 ± 1.98
24	gi|3914258|sp|P81243|PA21_BOTJA	Phospholipase A2 (Phosphatidylcholine 2-acylhydrolase) (BJ-PLA2)	7	<0.05
25	gi|17433168|sp|Q9PVE3|PA23_BOTAS	Phospholipase A2 homolog 3 precursor (Myotoxin III) (M1-3-3)	9	<0.05

†large standard deviation is mainly due to the effect of endogeneous proteolytic activities and degenerate peptides.

Table 4. Proteolytic and Sonoclot activities of venoms *C. s. scutulatus* A and B, *C. oreganus helleri* and *B. colombiensis*.

Venoms	MHD[‡] (µg)	MHemD[£] (µg)	Sonoclot ACT, CR, PF[€]	Fibrinogenolytic[∞] Crude Venom 2hr/24hr	Fibrinogenolytic[∞] Serine Free Venom 2hr/24hr
***C. s. scutulatus* A**[¶]	162.5	9.7	144, 10, 2.2	β/α,β	-/β
***C. s. scutulatus* B**[¶]	16	4.8	354, 6.2, 2.5	α,β/α,β	α/α,β
C. oreganus helleri	6	4.8	<26, >51, 1	α,β/α,β	α/α,β
B. colombiensis	25	2.4	<26, >51, 1	α,β/α,β	α,β/α,β

[¶] *C. s. scutulatus* A: neurotoxic venom; *C. s. scutulatus* B: hemorrhagic venom.
[‡]Minimal hemorrhagic dose: The amount of protein that will cause a 10 mm hemorrhagic spot.
[£]Minimal phospholipase A dose: The amount of protein that will cause a 10 mm halo.
[€]ACT (Activated Clot Time, sec): Time in which clot starts forming; CR: Clot Rate (clot signals/min); PF: Platelet Function. Normal control range values are: ACT: 128-213, CR: 15-26, PF: 3-5.
[∞]α,β: cleavage of alpha and beta chain; α: cleavage of alpha chain; -: no cleavage.

Table 5. Partial List of Protease Cleavage in the venom of *C.s. scutulatus* A and B for Putative venom metalloproteinase jararhagin precursor (HF2-proteinase) [Contains: Disintegrin]

Peptide Sequence[a]
P.VEDHCYYHGR.I
G.TPENCQNECCDAATCK.L
N.CQNECCDAATCK.
K.LKSGSQCGHGDCCEQCK.F
K.SGSQCGHGDCCEQCK.F
G.SQCGHGDCCEQCK.F
C.GHGDCCEQCK.F
G.HGDCCEQCK.F
C.RASMSECDPAEHCTGQSSECPADVFHK.N
R.ASMSECDPAEHCTGQSSECPADVFHK.N
R.ASMSECDPAEHCTGQSSECPADVFH.K
A.SMSECDPAEHCTGQSSECPADVFHK.N
M.SECDPAEHCTGQSSECPADVFHK.N
C.DPAEHCTGQSSECPADVFHK.N
D.PAEHCTGQSSECPADVFHK.N
P.AEHCTGQSSECPADVFHK.N
A.EHCTGQSSECPADVFHK.N
E.HCTGQSSECPADVFHK.N
T.GQSSECPADVFHK.N
K.NGQPCLDNYGY.C
K.NGQPCLDNYGYCYNGN.C
K.NGQPCLDNYGYCY.N
Q.KGNYYGYCR.K
K.GNYYGYCR.K
K.IPCAPEDVK.C
K.DNSPGQNNPCK.M
K.VCSNGHCVDVATA.Y
K.VCSNGHCVDVATAY.-

[a]Period indicates a tryptic cleavage site; dash indicates a C-terminal residue.

Table 6. Partial List of Protease Cleavage in the venom of *B. colombiensis* and *C. helleri* for Hemorrhagic metalloproteinase HT-D and HT-C precursor (Atrolysins D and C) (Hemorrhagic toxins C and D)

Peptide Sequence[a]
G.KITTNPSVEDHCYYR.G
K.ITTNPSVEDHCYYR.G
I.TTNPSVEDHCYYR.G
R.GRIENDADSTASISACNGLK.G
R.YIELVVVADHR.V
K.SHDNAQLLTAIELDEE.T
P.INLLMGVTMAHELGHNLGMEHDGKDCLR.G
L.MGVTMAHELGHNLGMEHDGKDCLR.G
M.GVTMAHELGHNLGMEHDGKDCLR.G
G.VTMAHELGHNLGMEHDGKDCLR.G
T.MAHELGHNLGMEHDGKDCLR.G
A.HELGHNLGMEHDGKDCLR.G
L.GHNLGMEHDGKDCLR.G
N.LGMEHDGKDCLR.G
G.MEHDGKDCLR.G
R.GASLCIMR.G
Y.KPQCILNKPLR.I

[a]Period indicates a tryptic cleavage site.

Figure Captions

Figure 1. Comparison between solid phase and SoPIL methods. MALDI-TOF MS was used to analyze a peptide mixture consisting of a cysteine-containing peptide laminin B (m/z 967.5) and a non cysteine-containing peptide angiotensin II (m/z 1046.6). (A) Prior to the reaction. (B) right after the addition of solid phase-$^{13}C_6$ beads (1 min); (C) right after the addition of the SoPIL-$^{12}C_6$ reagent (1 min); (D) Acid cleaved product from the one-step solid phase- $^{13}C_6$ and cleaved product from SoPIL-$^{12}C_6$ method. Ion of m/z 1100.6 is the product with light isotope tag, and ion m/z 1106.5 is the product with heavy isotope tag. The m/z 1046 ion was added for comparison.

Figure 2. Snake venom identification using SoPIL. Comparison of the protein composition of the venom from *C. scutulatus scuculatus* A and B and *C.o. helleri* and *B. colombiensis*

Figure 3. Quantitative analysis of SoPIL-labeled peptides.. (A) MS/MS spectrum of the peptide LTGC*DPTTDVYTYR (MH^+ 1738.6) from MTX-A. Its characteristic peptide bond fragment ions, type b and y ions, are labeled. (B) Reconstructed ion chromatogram of precursor ion (m/z 868.9) and its heavy version (m/z 871.9). Relative quantitation is performed using ASPARatio - that automatically integrates under the relevant regions of parent/single-ion trace chromatograms. The program draws a smoothed chromatogram based on the ion signal and then calculates the ratio of the peak areas. Raw

chromatograms are plotted in red, smoothed chromatograms in blue and areas used for calculating abundance ratio of the charge state in green.

Figure 4. Fibrinogenolytic activity of venoms at 2 and 24 hr. Ten microliters of whole (A, C) and serine free (B, D) venom (0.03 mg/mL) was added to 20 µL of fibrinogen solution (2.5 mg/mL) in 0.05 M Tris-HCl at pH 8.5 and incubated at 37 ˚C for 2 and 24 hr. Twenty four microliters of fibrinogen/venom fraction mixture was added to12 µL SDS buffer + 4 µL of reducing agent from Invitrogen® and boiled for 3 min. Twenty microliters of the mixture was added into the wells of 12% Tris-Glycine gels. Lanes: 1) Fibrinogen control; 2) *C. s. scutulatus* type A; 3) *C. s. scutulatus* type B; 4) *C. o. helleri;* and 5) *B. colombiensis*. Gels were run at 125 V, 40 mA for 1.5 hr using a Bio-Rad Basic Pac. Gels were stained with SimplyBlue™ SafeStain.

Figure 5. Sonoclot graph analysis of venoms on whole human blood. A glass bead activated test (gbACT + Kit obtained from Sienco, Inc.) was used to monitor activated clot time, clot rate and platelet function on a Sonoclot® Coagulation and Platelet Function Analyzer (Sienco, Inc.). A) Solid line: normal human blood control (no venom added); short dashed line: *C. s. scutulatus* B; long dased lines: *C. s. scutulatus* A, B) Solid line: normal human blood control; short dashed line: *C. o. helleri*; long dashed line: *B. colombiensis*.

References

1. Aebersold, R. (2003) Quantitative proteome analysis: methods and applications. *J Infect Dis* **187 Suppl 2**, S315-320
2. Ong, S. E., Foster, L. J., and Mann, M. (2003) Mass spectrometric-based approaches in quantitative proteomics. *Methods* **29**(2), 124-130
3. Duggan, D. J., Bittner, M., Chen, Y., Meltzer, P., and Trent, J. M. (1999) Expression profiling using cDNA microarrays. *Nat Genet* **21**(1 Suppl), 10-14.
4. Gygi, S. P., Corthals, G. L., Zhang, Y., Rochon, Y., and Aebersold, R. (2000) Evaluation of two-dimensional gel electrophoresis-based proteome analysis technology. *Proc Natl Acad Sci U S A* **97**(17), 9390-9395.
5. Old, W. M., Meyer-Arendt, K., Aveline-Wolf, L., Pierce, K. G., Mendoza, A., Sevinsky, J. R., Resing, K. A., and Ahn, N. G. (2005) Comparison of label-free methods for quantifying human proteins by shotgun proteomics. *Mol Cell Proteomics* **4**(10), 1487-1502
6. Li, X. J., Yi, E. C., Kemp, C. J., Zhang, H., and Aebersold, R. (2005) A software suite for the generation and comparison of peptide arrays from sets of data collected by liquid chromatography-mass spectrometry. *Mol Cell Proteomics* **4**(9), 1328-1340
7. Gygi, S. P., Rist, B., Gerber, S. A., Turecek, F., Gelb, M. H., and Aebersold, R. (1999) Quantitative analysis of complex protein mixtures using isotope-coded affinity tags. *Nat Biotechnol* **17**(10), 994-999.
8. Ross, P. L., Huang, Y. N., Marchese, J. N., Williamson, B., Parker, K., Hattan, S., Khainovski, N., Pillai, S., Dey, S., Daniels, S., Purkayastha, S., Juhasz, P., Martin, S., Bartlet-Jones, M., He, F., Jacobson, A., and Pappin, D. J. (2004) Multiplexed protein quantitation in Saccharomyces cerevisiae using amine-reactive isobaric tagging reagents. *Mol Cell Proteomics* **3**(12), 1154-1169
9. Schmidt, A., Kellermann, J., and Lottspeich, F. (2005) A novel strategy for quantitative proteomics using isotope-coded protein labels. *Proteomics* **5**(1), 4-15
10. Stewart, II, Thomson, T., and Figeys, D. (2001) 18O labeling: a tool for proteomics. *Rapid Commun Mass Spectrom* **15**(24), 2456-2465
11. Blagoev, B., Kratchmarova, I., Ong, S. E., Nielsen, M., Foster, L. J., and Mann, M. (2003) A proteomics strategy to elucidate functional protein-protein interactions applied to EGF signaling. *Nat Biotechnol* **21**(3), 315-318
12. Li, J., Steen, H., and Gygi, S. P. (2003) Protein profiling with cleavable isotope-coded affinity tag (cICAT) reagents: the yeast salinity stress response. *Mol Cell Proteomics* **2**(11), 1198-1204
13. Zhou, H., Ranish, J. A., Watts, J. D., and Aebersold, R. (2002) Quantitative proteome analysis by solid-phase isotope tagging and mass spectrometry. *Nat Biotechnol* **20**(5), 512-515.
14. van Heerbeek, R., Kamer, P. C., van Leeuwen, P. W., and Reek, J. N. (2002) Dendrimers as support for recoverable catalysts and reagents. *Chem Rev* **102**(10), 3717-3756
15. Tao, W. A., Wollscheid, B., O'Brien, R., Eng, J., Li, X., Bodenmiller, B., Watts, J., Hood, L., and Aebersold, R. (2005) Quantitative phosphoproteome analysis using

a dendrimer conjugation chemistry and mass spectrometry. *Nature Methods* **2**(8), 591-598
16. Guo, M., Galan, J., and Tao, W. A. (2007) A novel quantitative proteomics reagent based on soluble nanopolymers. *Chem Commun (Camb)* (12), 1251-1253
17. Farsky, S. H., Antunes, E., and Mello, S. B. (2005) Pro and antiinflammatory properties of toxins from animal venoms. *Curr Drug Targets Inflamm Allergy* **4**(3), 401-411
18. Marsh, N., and Williams, V. (2005) Practical applications of snake venom toxins in haemostasis. *Toxicon* **45**(8), 1171-1181
19. Bjarnason, J. B., and Fox, J. W. (1994) Hemorrhagic metalloproteinases from snake venoms. *Pharmacol Ther* **62**(3), 325-372
20. Barrett, A. J., and McDonald, J. K. (1986) Nomenclature: protease, proteinase and peptidase. *Biochem J* **237**(3), 935
21. Wolfsberg, T. G., and White, J. M. (1996) ADAMs in fertilization and development. *Dev Biol* **180**(2), 389-401
22. Harris, J. B. (1991) Phospholipases in snake venoms and their effects on nerve and muscle. *Snake Venoms.*, pp. 91-129
23. Kini, R. M. (2005) Serine proteases affecting blood coagulation and fibrinolysis from snake venoms. *Pathophysiol Haemost Thromb* **34**(4-5), 200-204
24. McLane, M. A., Sanchez, E. E., Wong, A., Paquette-Straub, C., and Perez, J. C. (2004) Disintegrins. *Curr Drug Targets Cardiovasc Haematol Disord* **4**(4), 327-355
25. Ruoslahti, E. (1996) RGD and other recognition sequences for integrins. *Annu Rev Cell Dev Biol* **12**, 697-715
26. Ritter, M. R., Zhou, Q., and Markland, F. S., Jr. (2000) Contortrostatin, a snake venom disintegrin, induces alphavbeta3-mediated tyrosine phosphorylation of CAS and FAK in tumor cells. *J Cell Biochem* **79**(1), 28-37
27. Lin, Y. T., Tang, C. H., Chuang, W. J., Wang, S. M., Huang, T. F., and Fu, W. M. (2005) Inhibition of adipogenesis by RGD-dependent disintegrin. *Biochem Pharmacol* **70**(10), 1469-1478
28. Zhou, Q., Nakada, M. T., Arnold, C., Shieh, K. Y., and Markland, F. S., Jr. (1999) Contortrostatin, a dimeric disintegrin from Agkistrodon contortrix contortrix, inhibits angiogenesis. *Angiogenesis* **3**(3), 259-269
29. Glenn, J. L., Straight, R. C., Wolfe, M. C., and Hardy, D. L. (1983) Geographical variation in Crotalus scutulatus scutulatus (Mojave rattlesnake) venom properties. *Toxicon* **21**(1), 119-130
30. Glenn, J. L., and Straight, R. C. (1989) Intergradation of two different venom populations of the Mojave rattlesnake (Crotalus scutulatus scutulatus) in Arizona. *Toxicon* **27**(4), 411-418
31. Sanchez, E. E., Galan, J. A., Powell, R. L., Reyes, S. R., Soto, J. G., Russell, W. K., Russell, D. H., and Perez, J. C. (2005) Disintegrin, hemorrhagic, and proteolytic activities of Mohave rattlesnake, Crotalus scutulatus scutulatus venoms lacking Mojave toxin. *Comp Biochem Physiol C Toxicol Pharmacol* **141**(2), 124-132
32. Fox, J. W., Ma, L., Nelson, K., Sherman, N. E., and Serrano, S. M. (2006) Comparison of indirect and direct approaches using ion-trap and Fourier

transform ion cyclotron resonance mass spectrometry for exploring viperid venom proteomes. *Toxicon* **47**(6), 700-714

33. Sanz, L., Gibbs, H. L., Mackessy, S. P., and Calvete, J. J. (2006) Venom proteomes of closely related Sistrurus rattlesnakes with divergent diets. *J Proteome Res* **5**(9), 2098-2112
34. Birrell, G. W., Earl, S. T., Wallis, T. P., Masci, P. P., de Jersey, J., Gorman, J. J., and Lavin, M. F. (2007) The diversity of bioactive proteins in Australian snake venoms. *Mol Cell Proteomics* **6**(6), 973-986
35. Bandeira, N., Clauser, K. R., and Pevzner, P. A. (2007) Shotgun protein sequencing: assembly of peptide tandem mass spectra from mixtures of modified proteins. *Mol Cell Proteomics* **6**(7), 1123-1134
36. Schwabacher, A. W., Lane, J. W., Schiesher, M. W., Leigh, K. M., and Johnson, C. W. (1998) Desymmetrization reactions: Efficient preparation of unsymmetrically substituted linker molecules. *Journal of Organic Chemistry* **63**(5), 1727-1729
37. Keller, A., Nesvizhskii, A. I., Kolker, E., and Aebersold, R. (2002) Empirical statistical model to estimate the accuracy of peptide identifications made by MS/MS and database search. *Anal Chem* **74**(20), 5383-5392.
38. Nesvizhskii, A. I., Keller, A., Kolker, E., and Aebersold, R. (2003) A statistical model for identifying proteins by tandem mass spectrometry. *Anal Chem* **75**(17), 4646-4658
39. Li, X., Zhang, H., Ranish, J. A., and Aebersold, R. (2003) Automated Statistical Analysis of Protein Abundance Ratios from Data Generated by Stable-Isotope Dilution and Tandem Mass Spectrometry. *Anal Chem* **75**(23), 6648-6657
40. Omori-Satoh, T., Sadahiro, S., Ohsaka, A., and Murata, R. (1972) Purification and characterization of an antihemorrhagic factor in the serum of Trimeresurus flavoviridis, a crotalid. *Biochim Biophys Acta* **285**(2), 414-426
41. Habermann, E., and Hardt, K. L. (1972) A sensitive and specific plate test for the quantitation of phospholipases. *Anal Biochem* **50**(1), 163-173
42. Glenn, J. L., and Straight, R. (1978) Mojave rattlesnake Crotalus scutulatus scutulatus venom: variation in toxicity with geographical origin. *Toxicon* **16**(1), 81-84
43. **R.C.Straight,** G. J. L. a. (1982) The rattlesnakes and their venom yield and lethal toxicity. In: A.T. Tu, Editor, Rattlesnake Venom: Their Actions and Treatment. 110
44. Mosquera, A., Idrovo, L. A., Tafur, A., and Del Brutto, O. H. (2003) Stroke following Bothrops spp. snakebite. *Neurology* **60**(10), 1577-1580
45. Salazar AM, R.-A. A., Girón ME, Aguilar I, Guerrero B. (2007) A comparative analysis of the clotting and fibrinolytic activities of the snake venom (*Bothrops atrox*)(serpentes:viperidae) from different geographical areas in Venezuela. *Thromb Res.* **20**(1), 95-104
46. Rodríguez-Acosta A, U. W., Azuaje R, Aguilar I, and Girón ME. (2000) A clinical and epidemiological analysis of accidental bites by snakes of the genus *Bothrops* in Venezuela. *Rev Cubana Med Trop* **52**, 90-94
47. Gutierrez, J. M., and Lomonte, B. (1995) Phospholipase A2 myotoxins from Bothrops snake venoms. *Toxicon* **33**(11), 1405-1424

48. Bober, M. A., Glenn, J. L., Straight, R. C., and Ownby, C. L. (1988) Detection of myotoxin alpha-like proteins in various snake venoms. *Toxicon* **26**(7), 665-673
49. Gopalakrishnakone, P., Dempster, D. W., Hawgood, B. J., and Elder, H. Y. (1984) Cellular and mitochondrial changes induced in the structure of murine skeletal muscle by crotoxin, a neurotoxic phospholipase A2 complex. *Toxicon* **22**(1), 85-98
50. Gralen, N., and Svedberg, T. (1938) The molecular weight of crotoxin. *Biochem J* **32**(8), 1375-1377
51. Metsch, R. B., Dray, A., and Russell, F. E. (1984) Effects of the venom of the Southern Pacific rattlesnake, Crotalus viridis helleri, and its fractions on striated and smooth muscle. *Proc West Pharmacol Soc* **27**, 395-398
52. Bush, S. P., and Siedenburg, E. (1999) Neurotoxicity associated with suspected southern Pacific rattlesnake (Crotalus viridis helleri) envenomation. *Wilderness Environ Med* **10**(4), 247-249
53. French, W. J., Hayes, W. K., Bush, S. P., Cardwell, M. D., Bader, J. O., and Rael, E. D. (2004) Mojave toxin in venom of Crotalus helleri (Southern Pacific Rattlesnake): molecular and geographic characterization. *Toxicon* **44**(7), 781-791
54. Sanchez, E. E., Galan, J. A., Perez, J. C., Rodriguez-Acosta, A., Chase, P. B., and Perez, J. C. (2003) The efficacy of two antivenoms against the venom of North American snakes. *Toxicon* **41**(3), 357-365
55. Ouyang, C., and Teng, C. M. (1976) Fibrinogenolytic enzymes of Trimeresurus mucrosquamatus venom. *Biochim Biophys Acta* **420**(2), 298-308
56. Meier, J., and Stocker, K. (1991) Effects of snake venoms on hemostasis. *Crit Rev Toxicol* **21**(3), 171-182
57. Braud, S., Bon, C., and Wisner, A. (2000) Snake venom proteins acting on hemostasis. *Biochimie* **82**(9-10), 851-859
58. Kini, R. M. (2004) Platelet aggregation and exogenous factors from animal sources. *Curr Drug Targets Cardiovasc Haematol Disord* **4**(4), 301-325
59. Markland, F. S. (1998) Snake venoms and the hemostatic system. *Toxicon* **36**(12), 1749-1800
60. Kornalik, F. (1991) *The influence of snake venom proteins on blood coagulation.*, Pergamon Press, New York
61. Kini, R. M., Rao, V.S. and Joseph, J.S. (2002) Procoagulant proteins from snake venoms. *Haemostasis* **31**, 218-224
62. Joseph, J. S., and Kini, R. M. (2004) Snake venom prothrombin activators similar to blood coagulation factor Xa. *Curr Drug Targets Cardiovasc Haematol Disord* **4**(4), 397-416
63. Aronson, D. L. (1976) Comparison of the actions of thrombin and the thrombin-like venom enzymes ancrod and batroxobin. *Thromb Haemost* **36**(1), 9-13
64. Bell, W. R., Jr. (1997) Defibrinogenating enzymes. *Drugs* **54 Suppl 3**, 18-30; discussion 30-11
65. Kini, R. M., Joseph, J.S., andd Rao, V.S. (2002) *Prothrombin activators from snake venoms.*, John Wiley, Chichester
66. Picotti, P., Aebersold, R., and Domon, B. (2007) The implications of proteolytic background for shotgun proteomics. *Mol Cell Proteomics* **6**(9), 1589-1598

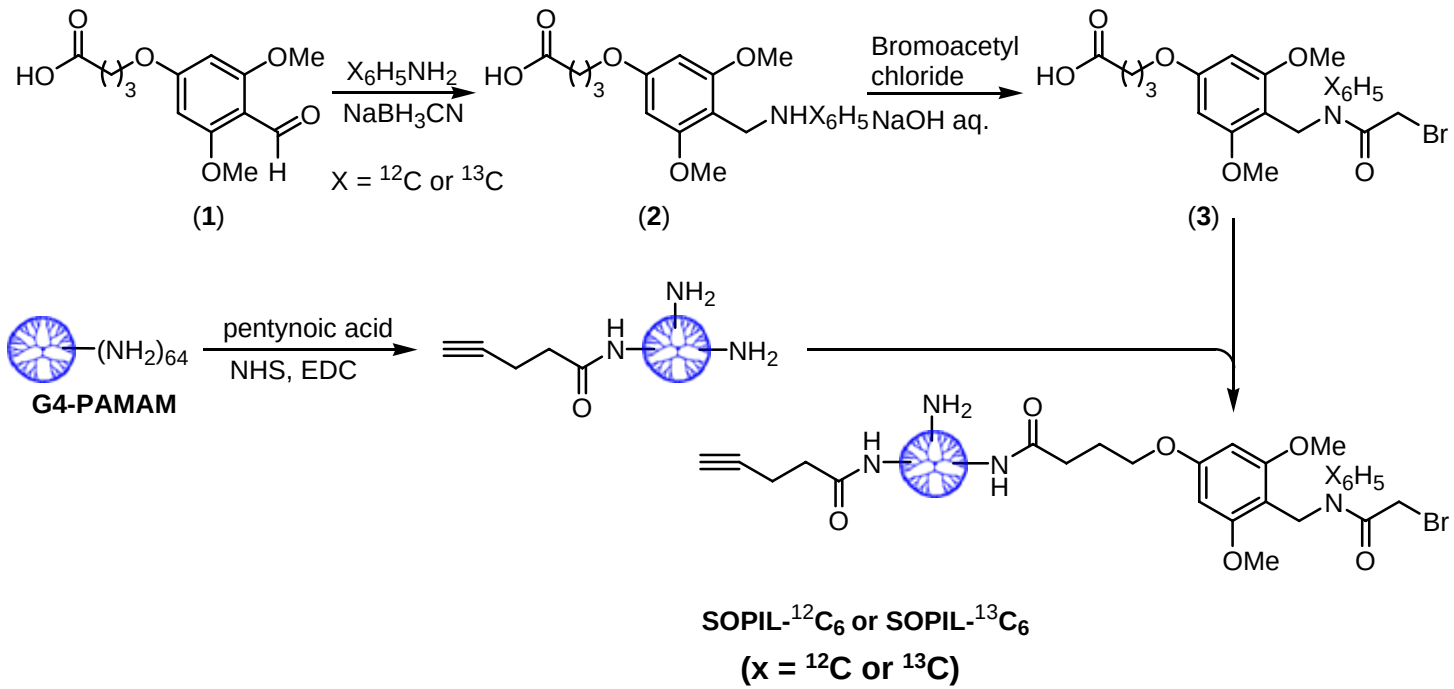

Scheme 1. Synthesis of SoPIL reagents.

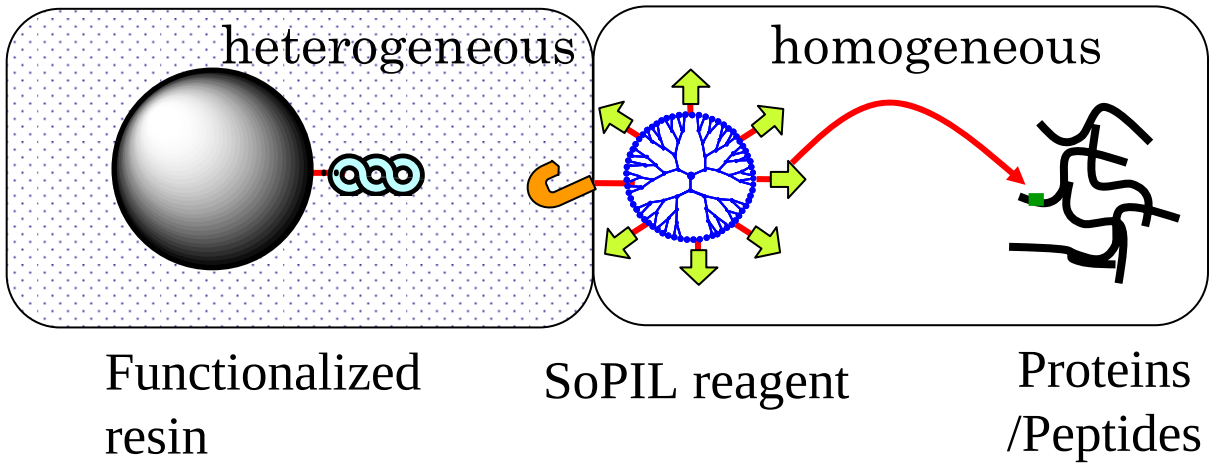

Scheme 2. Modular composition of the SoPIL strategy.

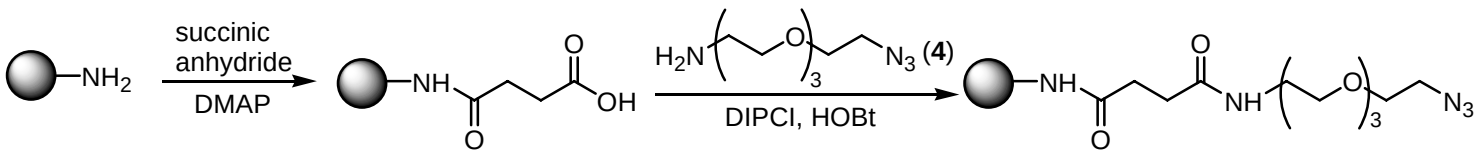

Scheme 3. Synthesis of azide beads.

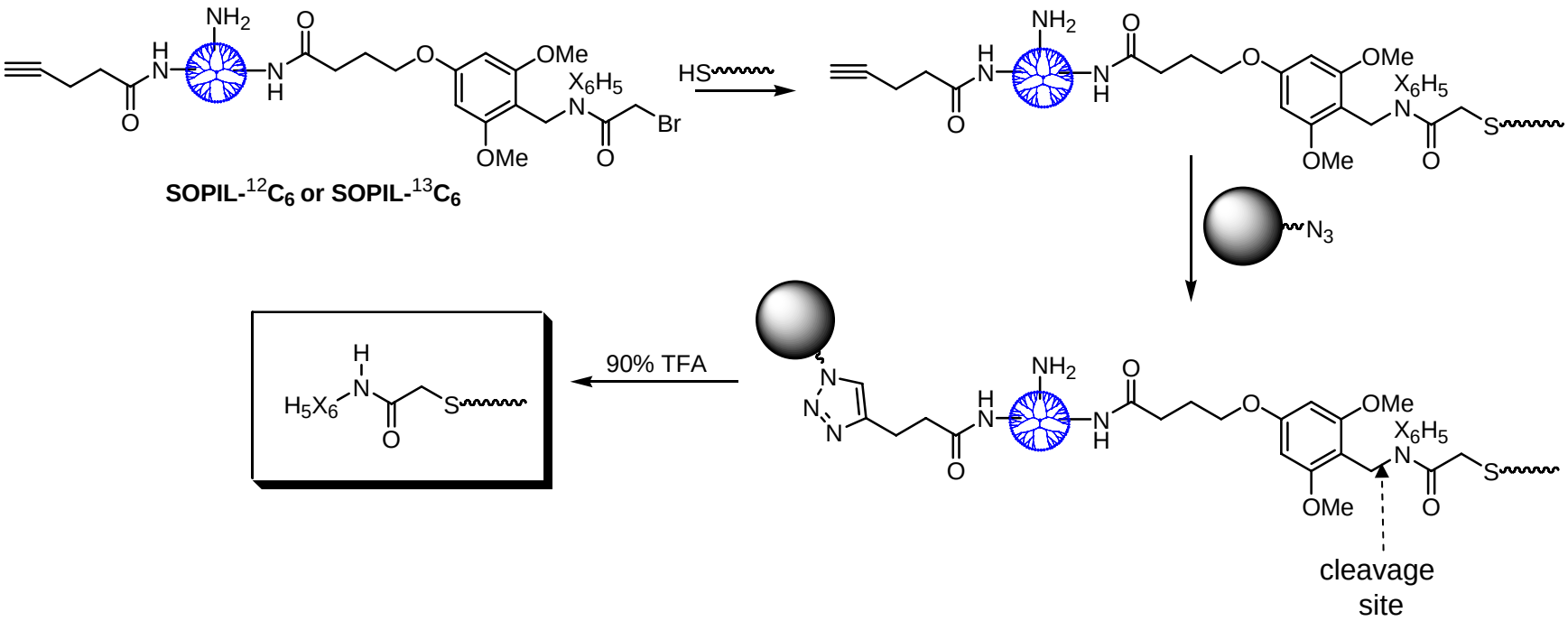

Scheme 4. Labeling Cys-containing peptides with SoPIL reagents.

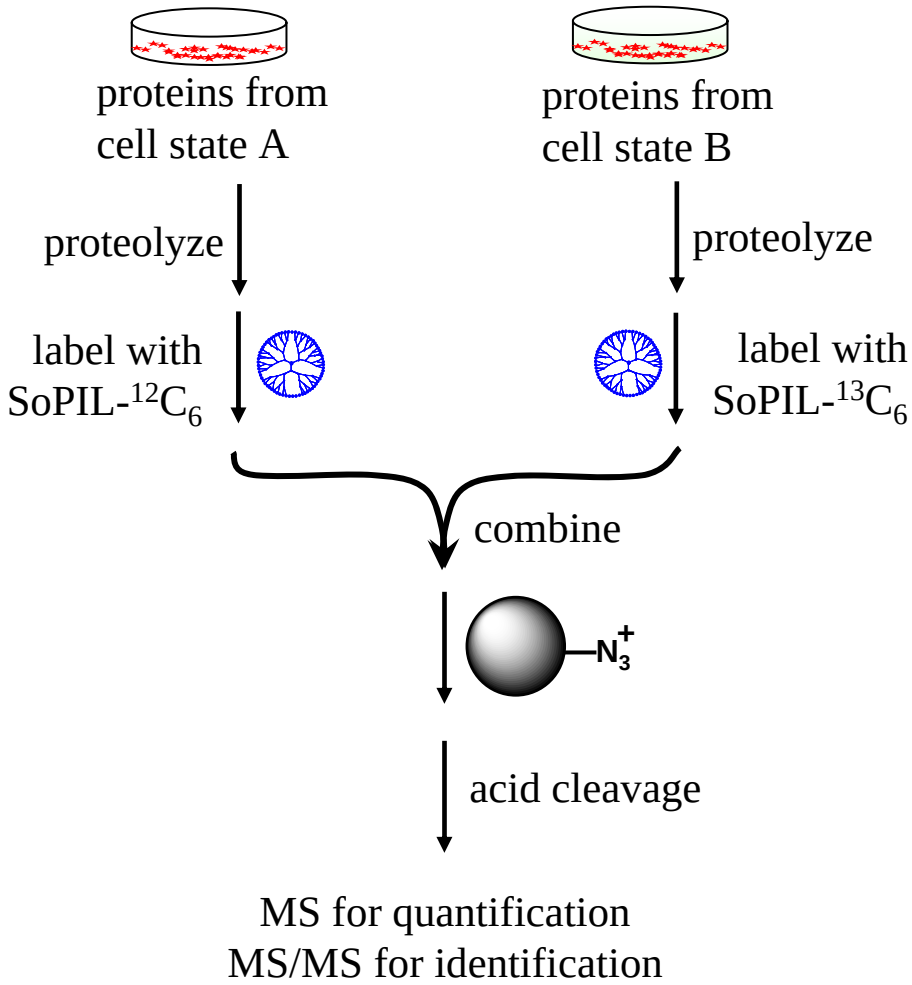

Scheme 5. Strategy for quantitative proteomics using SoPIL reagents.

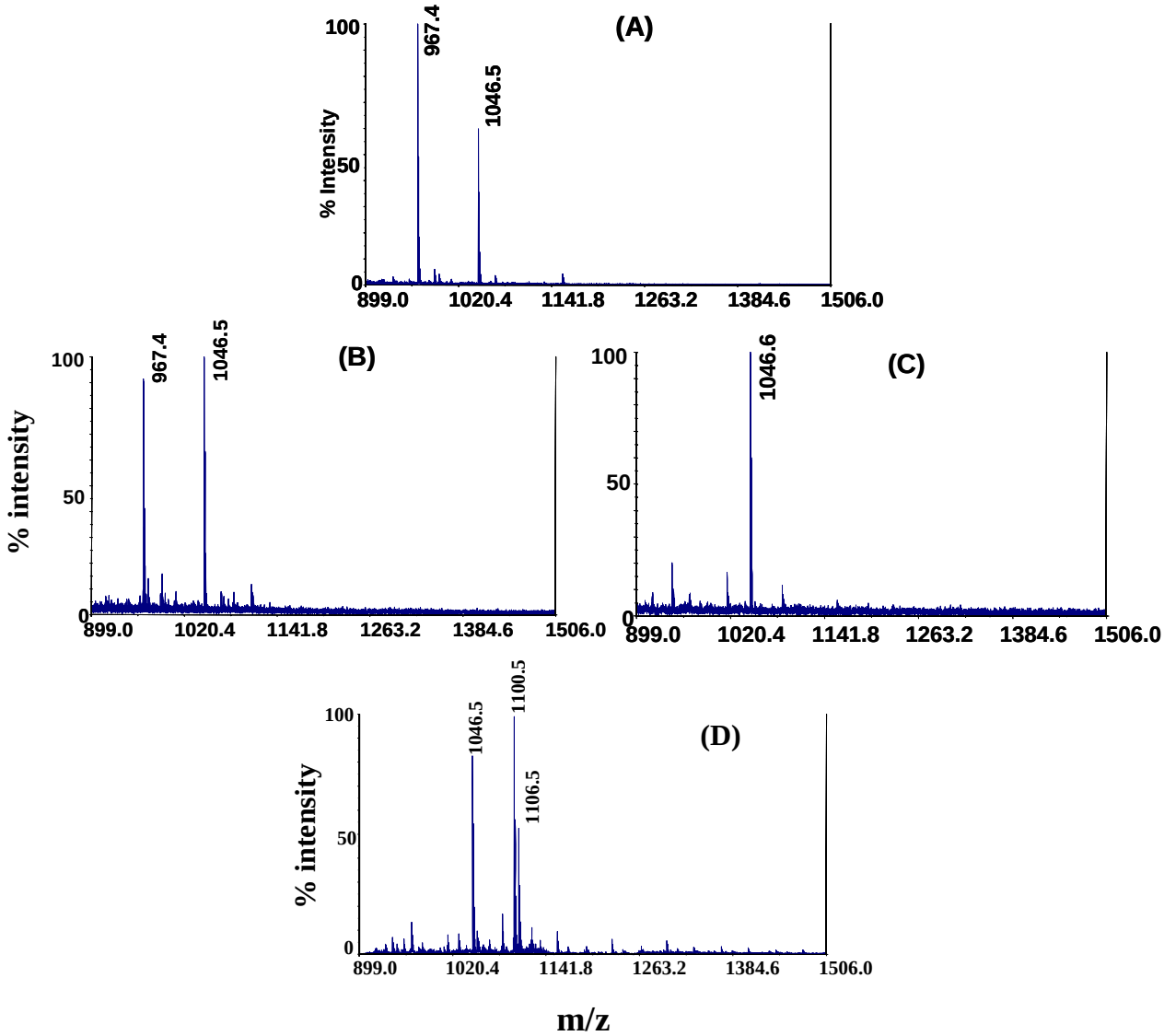
(A)
967.4
1046.5
% Intensity
100
50
0
899.0
1020.4
1141.8
1263.2
1384.6
1506.0
(B)
967.4
1046.5
% intensity
(C)
1046.6
(D)
1046.5
1100.5
1106.5
m/z

Figure 1

A)

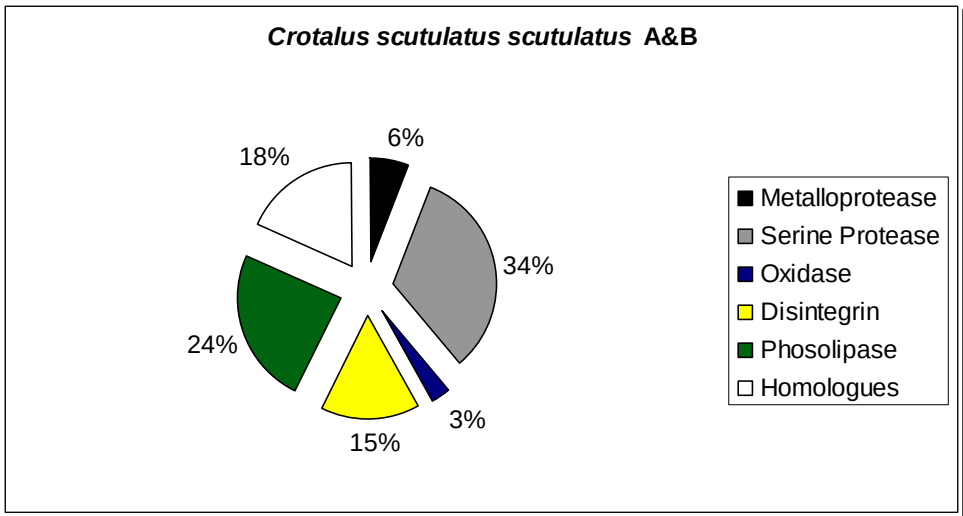

B)

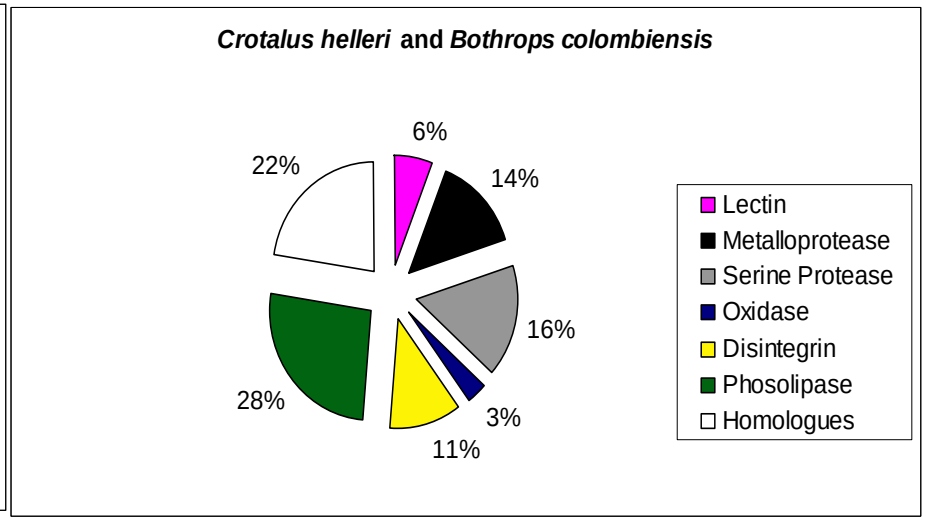

Figure 2 A&B

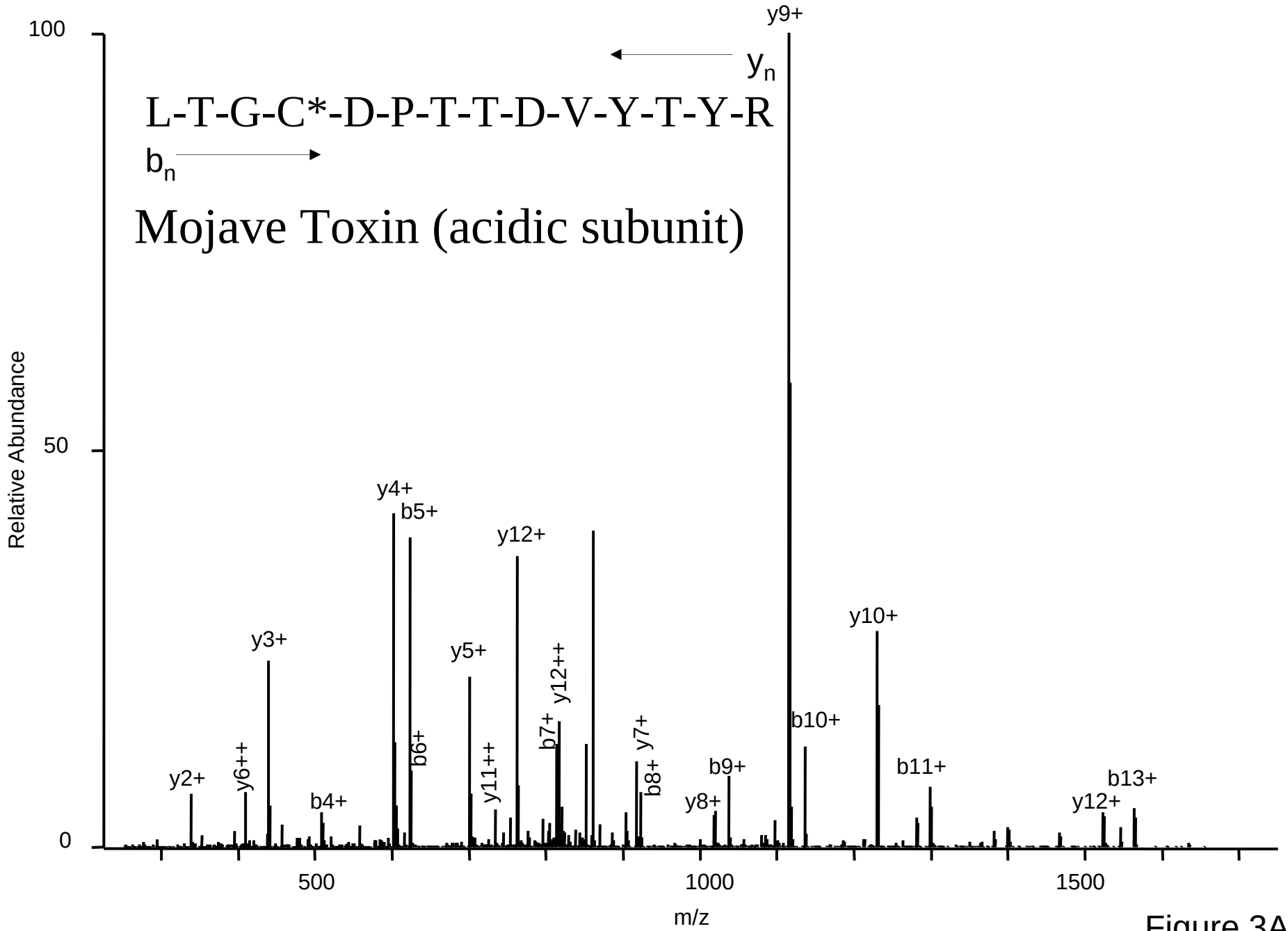
y9+
y_n
L-T-G-C*-D-P-T-T-D-V-Y-T-Y-R
b_n
Mojave Toxin (acidic subunit)
100
50
0
Relative Abundance
y4+
b5+
y12+
y3+
y5+
y12++
b10+
y10+
b6+
b7+
y7+
b8+
b9+
b11+
b13+
y2+
y6++
y11++
b4+
y8+
y12+
500
1000
1500
m/z

Figure 3A

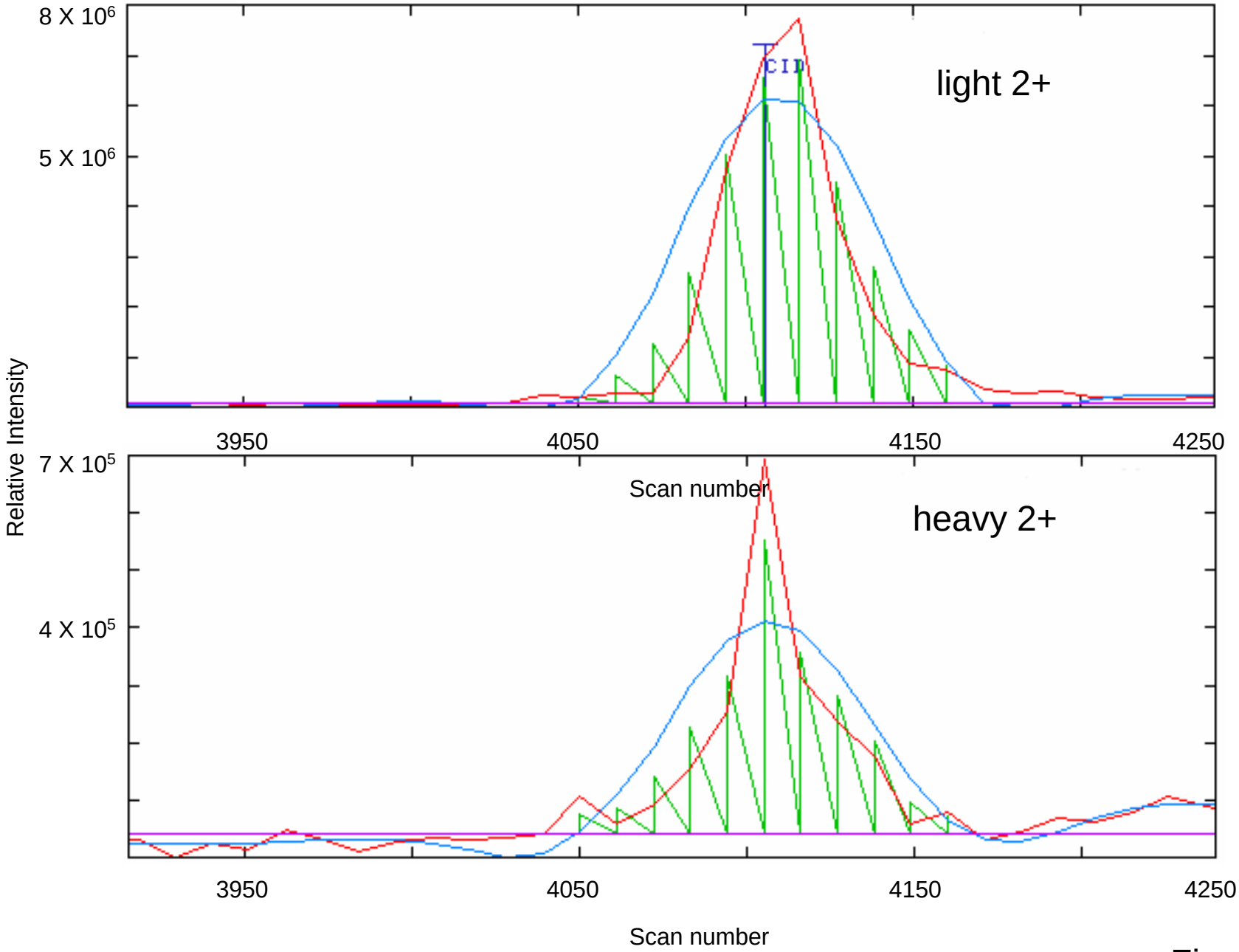
8 X 10^6
5 X 10^6
CID
light 2+
3950
4050
4150
4250
Relative Intensity
7 X 10^5
4 X 10^5
Scan number
heavy 2+
3950
4050
4150
4250
Scan number

Figure 3B

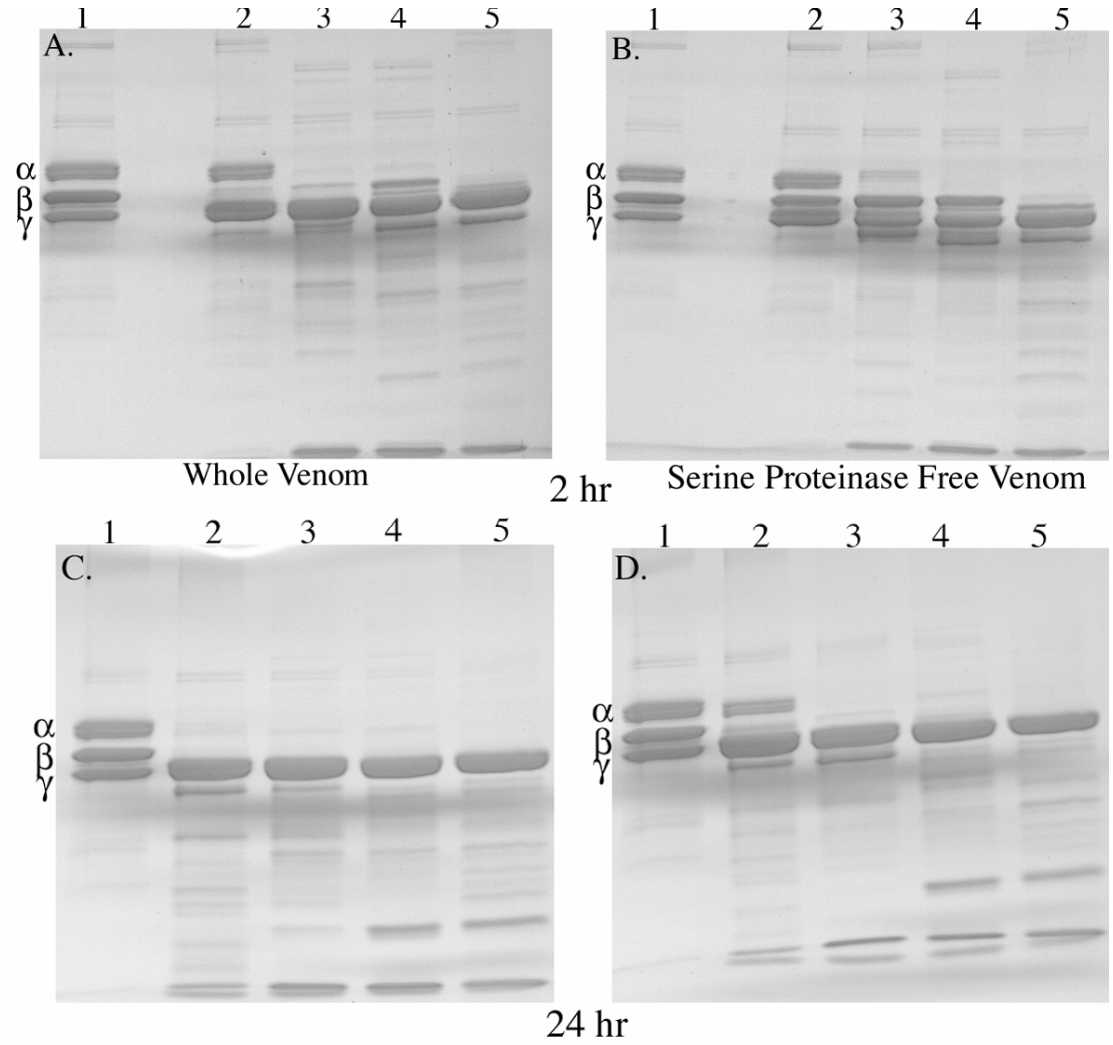

Figure 4 A,B,C,D

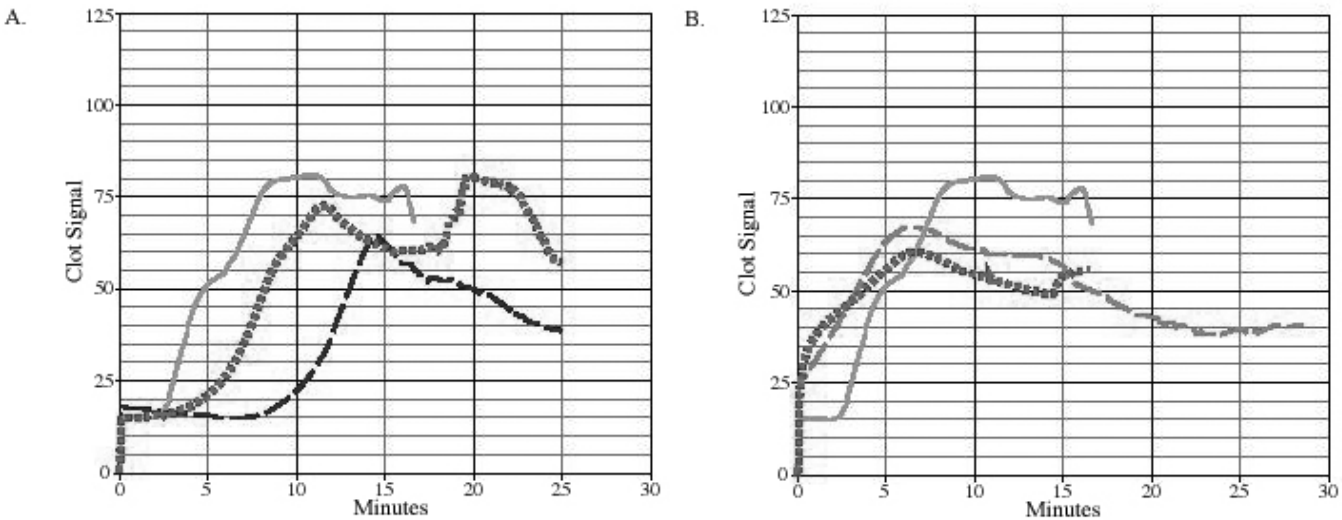

Figure 5 A&B